Resubmission of PR04-014 to PAC-26

Measurement of G_E^p/G_M^p using elastic $\vec{p}(\vec{e}, e'p)$ up to $Q^2 = 5.60$ (GeV/c)^2

May 24, 2004

J. Arrington, K. Hafidi, R.J. Holt, H.E. Jackson, D.H. Potterveld,
P.E. Reimer, E.C. Schulte, B. Zeidman, X. Zheng[1] (spokesperson)
Argonne National Laboratory, Argonne, IL 60439

P. Markowitz, J. Reinhold
Florida International University, Miami, FL 33199

W. Brooks, J.-P. Chen, R. Ent, D. Gaskell, D. Higinbotham, D. Mack, B. Reitz
Thomas Jefferson National Accelerator Facility, Newport News, VA 23606

S. Širca
University of Ljubljana, Slovenia

W. Bertozzi, O. Gayou, S. Gilad, P. Monaghan, Y. Qiang, L. Wan, Y. Xiao, C. Zhang
Massachusetts Institute of Technology, Cambridge, MA 02139

Z.-L. Zhou
Schlumberger-Doll Research, Ridgefield, CT 06877

W. Hersman, J.R. Calarco (co-spokesperson), M. Holtrop, T. Lee, H.-G.Zhu
University of New Hampshire, Durham, NH 03824

F. Wesselmann
Norfolk State University, Norfolk, VA 23504

R. Segel, I. Qattan
Northwestern University, Evanston, IL 60208

D.V. Jordan, J.I. McIntyre, B.D. Milbrath, G. Warren
Pacific Northwest National Lab, Richland, WA 99352

R. Gilman, X. Jiang, K. McCormick
Rutgers, The State University of New Jersey, Piscataway, NJ 08855

S. Choi, Z.-E. Meziani
Temple University, Philadelphia, PA 19122

G.D. Cates, D.G. Crabb, D. Day, N. Liyanage, P. Mckee,
O.A. Rondon (co-spokesperson), J. Singh, W.A. Tobias
University of Virginia, Charlottesville, VA 22904

[1]contact person, email: xiaochao@jlab.org

Abstract

We propose here measurements of the ratio G_E^p/G_M^p via doubly polarized elastic $\vec{p}(\vec{e},e'p)$ scattering at $Q^2 = 3.20$ and 5.60 (GeV/c)^2. The UVa polarized NH_3 target will be used in Hall C with its spin aligned at 41° and 80° w.r.t. the beam direction. To extract G_E^p/G_M^p, we perform measurements at kinematics where the elastic asymmetries are the most sensitive to this ratio. Assuming 75% beam polarization and 85 nA current, we request 17 days of beam time to achieve a precision of $\Delta(\mu G_E^p/G_M^p) = 0.063$ and 0.099 at $Q^2 = 3.20$ and 5.60 (GeV/c)^2, respectively. Here $\mu = \mu_p$ is the proton magnetic moment. We also request 6 days of overhead time.

Compared to PR04-014 where single-arm electron measurements were proposed, we propose here coincidence measurements with electrons detected by the large acceptance BETA detector and protons tagged by a large scintillator array. As a result the Q^2 range of this proposal is much higher than what was proposed in PR04-014.

The proposed measurement will provide the first data on G_E^p/G_M^p from the $\vec{p}(\vec{e},e'p)$ asymmetry method in the region $Q^2 > 3$ (GeV/c)^2 with good precision. It represents the next step in a logical scientific progression to fully understand the discrepancy between data from the Rosenbluth separation and the polarization transfer technique. One possible explanation of this observed discrepancy is the two-photon exchange correction, which so far is difficult to study experimentally in region $Q^2 > 2$ (GeV/c)^2. The direct extraction of G_E^p/G_M^p from the double polarization asymmetry is expected to be less sensitive to the two-photon exchange effect than the Rosenbluth separation. Moreover, so far almost all calculations on the two-photon exchange correction use the observed discrepancy itself as an input, or assume that the polarization transfer data give the true values of G_E^p/G_M^p. It is therefore critical to provide an independent check of polarization transfer data before spending extensive effort on studying the details of the two-photon exchange effect. The new method proposed here serves this purpose perfectly – while based on the same double polarization principles, it has completely different systematic uncertainties than the polarization transfer method. In particular, it does not suffer from the uncertainties due to particle spin precession in the spectrometer. Finally, in addition to the two-photon exchange, there might be other processes of which we are not aware that can contribute to the discrepancy. The new data will give an opportunity to explore such unknown effects.

Contents

1 Motivation **4**
- 1.1 Theories . . . 4
- 1.2 Existing Data . . . 4
- 1.3 Two-Photon Exchange Correction . . . 6

2 The Proposed Experiment **8**

3 Experimental Setup **9**
- 3.1 Overview . . . 9
- 3.2 Beam Line . . . 9
- 3.3 The UVa NH_3 Target . . . 12
- 3.4 The BETA detector . . . 15
- 3.5 The Scintillator Array . . . 16
- 3.6 Acceptance Matching and the Effect of the Target . . . 19
- 3.7 Data Analysis . . . 20

4 Expected Uncertainties and Rate Estimation **21**
- 4.1 Experimental Systematics . . . 21
- 4.2 Beam Charge Asymmetry . . . 21
- 4.3 Target Polarization . . . 21
- 4.4 Target Dilution Factor . . . 21
- 4.5 Nitrogen Asymmetry . . . 23
- 4.6 Background . . . 24
- 4.7 Electromagnetic Radiative Corrections . . . 25
- 4.8 Deadtime Correction . . . 25
- 4.9 Optimization of Kinematics . . . 25
- 4.10 Summary of Rate and Expected Uncertainties . . . 25

5 Beam Time Request **29**

6 Comparison to PR04-014 **29**

7 Summary **29**

A Doubly Polarized Elastic Scattering **30**

B Error Propogation of Systematic Uncertainties for G_E^p/G_M^p **31**

C PAC-25 report for PR04-014 **33**

1 Motivation

The nucleon is one of the basic building blocks of nature. The elastic form factors are important fundamental properties of the nucleon, describing its internal structure due to the spatial distribution of its charge and magnetism, and play an essential role in hadronic physics as the *sine qua non* input to our understanding of the nucleon structure. Thus it is of the utmost urgency that we have accurate and reliable measurements of these fundamental qualities of the nucleon from low Q^2 to the highest Q^2 we can reach. However, there is a discrepancy between the proton G_E/G_M data obtained by two very different techniques that clearly indicates a problem in either the experimental methods or the theoretical basis used to extract the form factors from the data. Any such discrepancies must be resolved without delay. In this proposal, we propose an independent measurement of the ratio G_E/G_M on the proton using a third technique which is experimentally unrelated to either of the first two. In this Section we will first briefly review available calculations for G_E^p/G_M^p, then give an overview of previous world data, summarize the current status of theoretical and experimental studies of the two-photon exchange effect, and in the end propose a new method to measure the G_E^p/G_M^p ratio.

1.1 Theories

The proton elastic form factors have been calculated in various models. At low four momentum transfer squared $Q^2 < 1$ (GeV/c)^2, the Vector Meson Dominance (VMD) model [1] successfully describes the nucleon form factors. In the high Q^2 region, the dominant degrees of freedom of the nucleon are the three valence quarks and perturbative Quantum Chromo-Dynamics (pQCD) can be applied [2]. Specifically, based on the leading-order pQCD, or hadron helicity conservation, the ratio of Dirac and Pauli form factors F_2^p/F_1^p is expected to scale as $1/Q^2$ at high Q^2 [2, 3], which directly constrains the behavior of G_E^p/G_M^p in this region.

In the intermediate region $1 < Q^2 < (10-20)$ (GeV/c)^2 (or higher), however, predictions for the nucleon form factors become difficult because the soft scattering processes are still dominant compared to hard scattering. Moreover, these soft contributions might be different for different observables of the scattering processes. This fact itself can be used as a tool to understand the role of the soft processes without reaching asymptotically high Q^2. Many QCD models have been used to calculate the elastic nucleon form factors in this region - the relativistic constituent quark model (RCQM) [4, 5], the cloudy bag model (CBM) [6], the SU(6) breaking CQM [7], the point-form spectator approximation (PFSA) model based on the Goldstone boson exchange CQM [8], and the chiral soliton model [9]. Figure 1 shows existing calculations for $\mu G_E^p/G_M^p$ along with world data, where $\mu = \mu_p = 2.793\mu_N$ is the proton magnetic moment.

1.2 Existing Data

The proton elastic form factors have been measured for almost five decades. In the traditional Rosenbluth separation method, based on the assumption of the one-photon exchange process, the elastic cross section is measured at fixed Q^2 but different values of the virtual photon polarization ε. Then the values of G_E^p, G_M^p and their ratio are extracted from a linear fit of the cross section as a function of ε. Data from this method show that G_M^p can be approximated by the dipole form $G_D = \mu/(1+Q^2/0.71)^2$, at least up to about $Q^2 = 3-4$ (GeV/c)^2. The ratio $\mu G_E^p/G_M^p$ is observed by this method to be close to unity. Above this Q^2 region, G_M^p is extracted from single cross section measurements assuming $\mu G_E^p = G_M^p$. Data on F_1^p at $Q^2 > 10$ (GeV/c)^2 show a $1/Q^4$ scaling behavior which is consistent with pQCD predictions [10].

However, recent data from the method of measuring the polarization transfer [12, 13, 14] showed that $\mu G_E^p/G_M^p$ drops linearly as Q^2 increases and reaches as low as ≈ 0.3 at $Q^2 = 5.6$ (GeV/c)^2, in significant disagreement with the Rosenbluth data (see Fig. 1). This dramatic change has provoked large

Figure 1: Previous world data for $\mu G_E^p/G_M^p$ from a global analysis of Rosenbluth data [11] (open squares) and from polarization transfer method [12, 13, 14] (open and solid stars). A dramatic disagreement is clearly seen between the two data sets at $Q^2 > 2$ (GeV/c)^2. Preliminary results from a recent Hall A high precision Rosenbluth experiment (solid squares) [17] agree with previous Rosenbluth data. Curves are calculations from VMD (black) [1], RCQM (red) [5], SU(6) breaking with CQM FF (blue) [7], PSFA (green) [8] and chiral soliton model (magenta) [9].

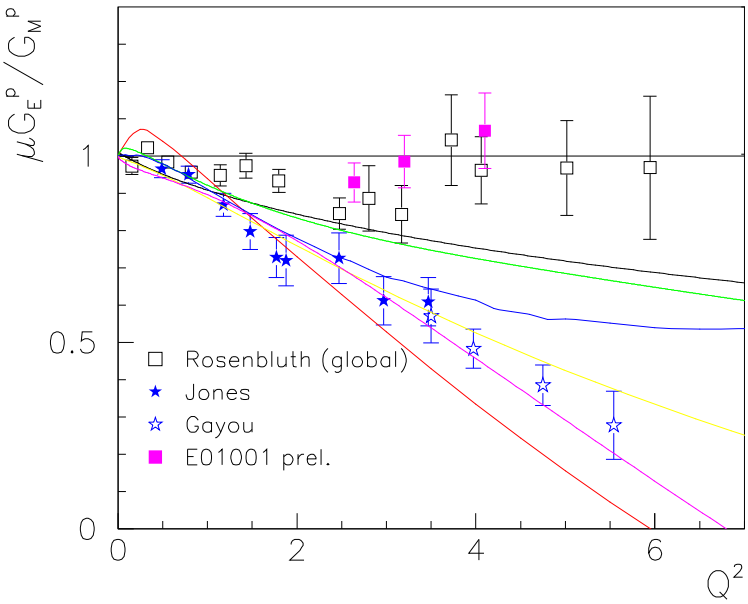

interest in both theoretical and experimental aspects of the proton form factor studies. Different fits have been performed separately to cross section data, and data from both cross section measurements and polarization transfer methods [15]. Previous Rosenbluth data have been re-analyzed [16] but the results are still inconsistent with polarization measurements. At high Q^2, data from cross section measurements have also been re-analyzed [16] using the polarization transfer fit [13].

Experimentally, preliminary results from the recently completed Hall A high precision Rosenbluth experiment E01-001 [17] agree well with previous Rosenbluth data. A new polarization transfer experiment [18] is planned in Hall C to measure $\mu G_E^p/G_M^p$ up to $Q^2 = 9.0$ (GeV/c)^2. Since a new proton polarimeter will be used in a spectrometer different from what was used in previous experiments, it is expected to check the systematic uncertainties of existing polarization transfer data, especially those due to the uncertainty of the spin precession. However the new experiment is still based on the same technique and analyzing methods as previous polarization transfer experiments, so it will still share some of the systematics. Therefore, it is critical to have a fully independent double polarization experiment, and this is *the* main purpose of this proposal.

1.3 Two-Photon Exchange Correction

In order to explain the discrepancy between the Rosenbluth separation and polarization transfer data, assuming that both are correct, significant effort has been spent on the understanding of radiative corrections and soft processes that can modify the results obtained under the assumption of one-photon exchange. The validity of radiative corrections has been checked, and it has been suggested that the two-photon exchange process may explain part of the discrepancy between the two data sets.

Earlier data on the ratio of the $e^+ - p$ and $e^- - p$ scattering cross sections indicated that the two-photon exchange correction was small [19]. As a result, when analyzing the Rosenbluth data, the two-photon (and higher order) exchange corrections were small in the traditional radiative corrections [20].

On the other hand, if this correction is not small, it can introduce an ε-dependence to the cross section and effect the linearity of the Rosenbluth plot. Guichon and Vanderhaeghen [21] showed that, based on general forms of this correction, the effect on the Rosenbluth data is much larger than that on the polarization transfer data, and the true $\mu G_E^p/G_M^p$ is about 20% below the fit to polarization transfer data. Blunden, Melnitchouk and Tjon [22] evaluated the two-photon exchange contributions to elastic $e - p$ scattering cross sections based on a simple hadronic model including the finite size of the proton. Their results explained one third of the discrepancy between the two data sets.

Rekalo and Tomasi-Gustaffson [23] derived from first principles, *i.e.* the C-invariance of the EM interaction and the crossing symmetry, the general properties of two-photon exchange in $e - p$ elastic scattering. They showed that the presence of this mechanism destroys the linearity of the Rosenbluth separation but does not significantly affect the terms related to the EM form factors.

In a recent work by Chen *et al.*, the two-photon exchange contribution was estimated for elastic $e - p$ scattering where the scattering occurs from a parton in the proton [24]. The process on the nucleon was related to the generalized parton distributions. It was found that *if using the polarization transfer data as the proton form factors*, then when adding in the two-photon correction to the polarization transfer data, it is possible to reproduce the Rosenbluth data to a certain level. In Fig. 2, we show data on the reduced cross section $\sigma_R = \tau G_M^2 + \varepsilon G_E^2$ at $Q^2 = 3.2$ and 4.1 (GeV/c)^2 from a recent high precision Rosenbluth experiment in Hall A (black points) [17]. The ε-dependence of σ_R is fit by the solid line. Then we add in the two-photon correction of Chen's work, the corrected σ_R are shown as green (using corrections at

Figure 2: Data on the reduced cross section σ_R at $Q^2 = 3.2$ (left) and 4.1 (GeV/c)^2 (right) from a recent Hall A high precision Rosenbluth experiment (black points) [17]. After adding in the two-photon correction by Chen *et al.* [24], the corrected σ_R (green points if using corrections at $Q^2 = 2.5$ (GeV/c)^2, and red points if using $Q^2 = 5$(GeV/c)^2 corrections) fall half-way between the uncorrected Rosenbluth data (fit by black line) and a fit to polarization transfer data (blue dashed line).

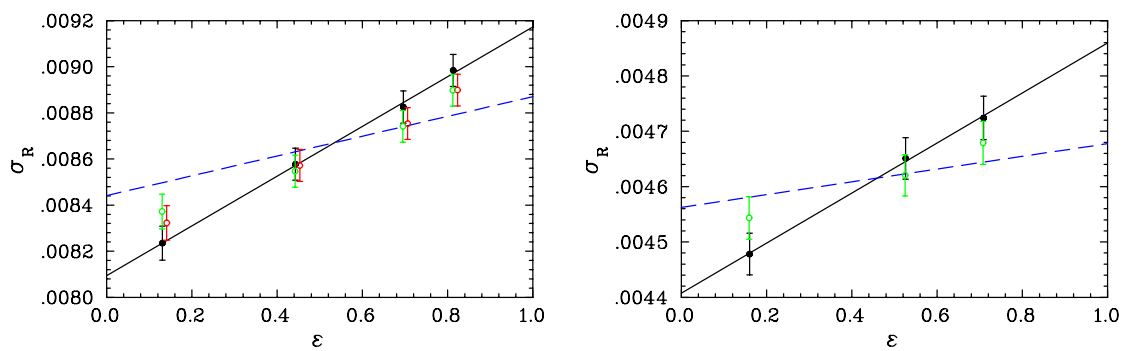

$Q^2 = 2.5$ GeV^2) and red points (using corrections at $Q^2 = 5$ GeV^2). The blue dashed line shows the slope of σ_R if G_E/G_M ratio agrees with the polarization transfer data. Apparently, at both Q^2 values, this calculation explains at most half of the discrepancy.

The double polarization experiment, on the other hand, provides a more direct measurement of the ratio $\mu G_E/G_M$. The calculations show that the two-photon contributions are small to both the transverse and the longitudinal polarization transfer components P_t and P_l [21, 22, 25]. Figure 3 shows results of one of the calculations [26]. Therefore, while the ratio $\mu G_E/G_M$ from the spin transfer measurement will

Figure 3: Two-photon corrections for P_t and P_l at $Q^2 = 3.0$ (left) and 5.0 (GeV/c)^2 (right), from one of the calculations [26]. Here $P_{t,l}(1\gamma)$ is the polarization transfer component from only the one-photon exchange and $P_{t,l}(1\gamma + 2\gamma)$ is the contribution from both one- and two-photon exchanges. In the region $\varepsilon > 0.7$ at both Q^2 values, the two-photon correction is no larger than 3% for either component.

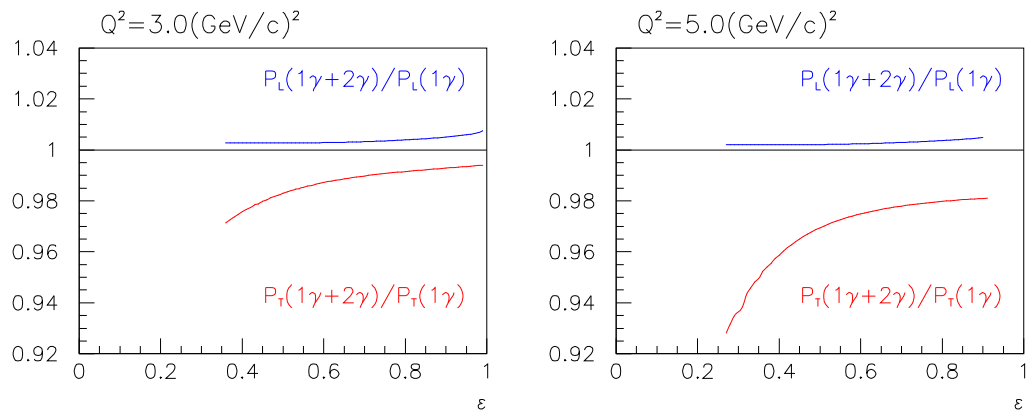

be affected by the two-photon exchange contributions, the size of the effect is expected to be much less than for the Rosenbluth separation technique and may be within experimental uncertainties for the higher Q^2 data points. The same is true for the asymmetries of doubly polarized elastic scattering.

Armed with the prediction that the two-photon exchange could be large, earlier SLAC data on the ratio of the $e^+ - p$ and $e^- - p$ scattering cross sections have been re-examined to see if the two-photon exchange effects on the cross section may explain the discrepancy in $\mu G_E^p/G_M^p$ data. It has been shown that there is indeed a hint that the two-photon exchange correction is large [27]. In this context, it is interesting to see how people's opinion changes with time – what we believed forty years ago turns out to be incorrect and those important measurements (e^+ scattering in this case) were abandoned just because they were *supposed* to give the same results as other measurements (e^- scattering). Fortunately effort has been started recently on measuring precisely the ε-dependence of the $e^+ - p$ to $e^- - p$ cross section ratio up to $Q^2 \approx 1.5$ (GeV/c)^2 using the near-4π detector CLAS [28]. Since this is the only direct method to measure the two-photon effect contribution to the discrepancy in proton form factor data, one may have a more solid answer about the two-photon contribution in this Q^2 region in the near future. But even if this experiment is completed, the data (including all existing e^+ data) are all in a low Q^2 region $\lesssim 2$ (GeV/c)^2 and it will be difficult to set a good limit on the two-photon correction for higher Q^2.

Alternate investigations of the two-photon exchange effect are possible. For example, one can measure the non-linearity of the Rosenbluth plot [29] and check two-photon exchange calculations. It was also predicted [30, 31] that the interference between the one- and two-photon exchange processes leads to a non-zero asymmetry A_N for target polarized transversely to the scattering plane. An early attempt

to measure this at SLAC showed the asymmetry to be zero but within rather large uncertainties [32]. There has been a recent suggestion to measure this asymmetry using BLAST at the MIT-Bates accelerator facility, and an experiment was proposed for Hall C [33]. Other possibilities include a measurement of the transverse beam asymmetry A_y. Such data exist at very low Q^2, around 0.1 (GeV/c)^2, from the MAINZ-A4 and the SAMPLE experiments [34]. However, such measurements are doubly difficult: they require very high precision data on either cross sections (Rosenbluth linearity check), or on asymmetries (A_T) over a wide kinematic (ε) range and the development of new experimental facilities (transversely polarized target for A_N, or special designed polarimeter for P_N). Moreover, they are sensitive to either only the non-linear part, or only the imaginary part of the two-photon exchange effect. In one word, we can not expect that any of these methods will directly solve the proton form factor discrepancy.

The two-photon exchange correction provides a possible explanation of the discrepancies in the existing data. Furthermore it not only affects the extraction of form factors from $e-p$ scattering, but also affects many other observables, *e.g.* parity-violating asymmetries. A full understanding of this process may take many years, and a large amount of experimental study is necessary to provide guidance to theoretical work. We also cannot exclude the possibility that there might be other corrections, which we are not aware of, that add to the discrepancy between the two form factor data sets. Hence it might not be appropriate to attribute the full discrepancy to two-photon exchange effects. In this sense, it is critical to perform an independent determination of $\mu G_E/G_M$ from double polarization observables to check the results from the polarization transfer data, before significant efforts are spent on the study of two-photon exchange effects.

2 The Proposed Experiment

We propose here a third method to measure G_E^p/G_M^p in the intermediate Q^2 range at 3.20 and 5.60 (GeV/c)^2. We will measure the double polarization asymmetry in $\vec{e}-\vec{p}$ elastic scattering and the G_E^p/G_M^p ratio will be extracted from the measured asymmetries. The first (and maybe the only) measurement of G_E^p/G_M^p using this method was performed at SLAC in the 1970's [35] and the result was used to determined the sign of G_E/G_M for the proton. The method of using double polarization asymmetry of muon scattering to study the nucleon EM form factors was also discussed in the literature [36]. Formulas for doubly polarized elastic scattering and its asymmetries are given in Appendix A.

For the proposed measurement, the UVa polarized NH_3 target will be used in Hall C with its spin aligned at 41° and 80° w.r.t. the beam-line, pointing to the left of the beam-line when viewing toward beam dump. The scattered electrons will be detected in the BETA detector and protons in a scintillator array. Assuming 85 nA beam current with 75% polarization, we request 17 days of 5.552 GeV beam to reach an uncertainty $\Delta(\mu G_E^p/G_M^p) = 0.063$ and 0.099 at $Q^2 = 3.20$ and 5.60 (GeV/c)^2, respectively. Six days overhead time are needed for commissioning of the equipment and target work.

The proposed measurement will provide the first precision data on $\mu G_E^p/G_M^p$ from a third method in the intermediate Q^2 range. This method is expected to be less sensitive to the two-photon exchange effect than Rosenbluth separation, based on the same argument as for the polarization transfer method that they are both direct measurements of $\mu G_E^p/G_M^p$. Furthermore, it has different systematic uncertainties compared to the polarization transfer technique. Hence, it will complement these two methods. The new results will provide crucial information on both the proton structure and the understanding of previous world data, and provide reliable guidance for theoretical work on two-photon exchange corrections.

3 Experimental Setup

In the following we describe the experimental setup for the proposed measurement in Hall C.

3.1 Overview

The floor plan for Hall C is shown in Fig. 4 (schematic) and Fig. 5 (drawing). The UVa polarized NH_3 target will be installed with its spin direction aligned at $41°$ and $80°$ w.r.t. the beam-line, as shown in

Figure 4: Hall C floor plan for the proposed measurement (not to scale).

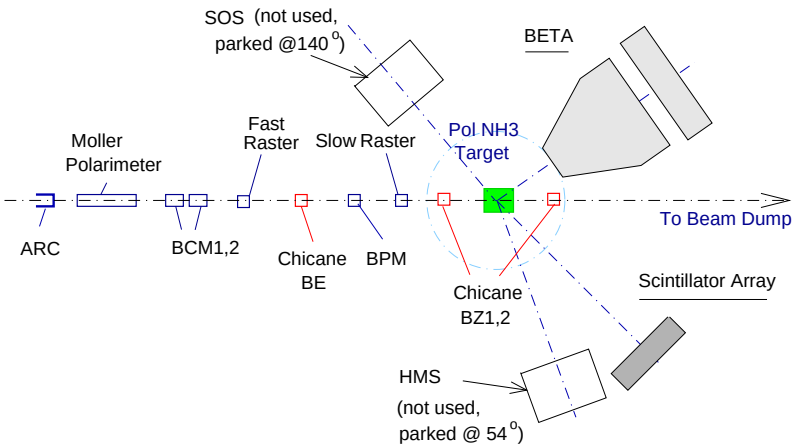

Fig. 6. The scattered electrons will be detected by the BETA (Big Electron Telescope Array) installed on the left side of the beam-line. A scintillator array will be assembled and installed on the right side of the beam-line to detect scattered protons. Elastic events are identified by the electron scattering angle and momentum, and triggering of the proton events in the scintillator array. Coplanary conditions will be applied on the proton scattering angle to suppress quasi-elastic events and other backgrounds. Because scattered particles will be deflected by the target field, both BETA and the scintillator array need to be installed out-of-plane. The HMS and the SOS will not be used and will be parked at $54°$ and $140°$, respectively. A new target platform needs to be built to accommodate the large parking angle of the HMS. In Fig. 5, the cryo-line of the HMS hits some of the instruments on the current target platform.

3.2 Beam Line

We propose to use 5.552 GeV polarized electrons with 75% polarization and 85 nA beam current. Beam energy will be measured to $\Delta E/E = 5 \times 10^{-4}$ level using the ARC method [37]. We plan to use the Møller polarimeter for beam polarization measurement. Currently the Hall C Møller polarimeter can provide better than 1% precision. However additional systematic error can come from the leakage from other halls during Moller measurements. We therefore use 1.5% in the uncertainty estimation.

Because the target spin is not parallel to the beam direction, the strong 5 T magnetic field of the target will bend the electron beam toward the floor. In order to ensure that the incoming beam is incident on the target cell horizontally, we will use Hall C's BE and BZ1 chicane magnets to bend the beam up before it

Figure 5: Design of Hall C floor layout for the proposed measurement. In this drawing, the Čerenkov and Lucite hodoscope sector of the BETA is at 83 cm and the calorimeter sector is at 7 m away from the target. The Scintillator array is 1.6m(H)×1.6m(W) at 5 m away from the target. The HMS and the SOS are parked at 54° and 140°, respectively. The target platform is the old design and overlay underneath the HMS cryogenic lines.

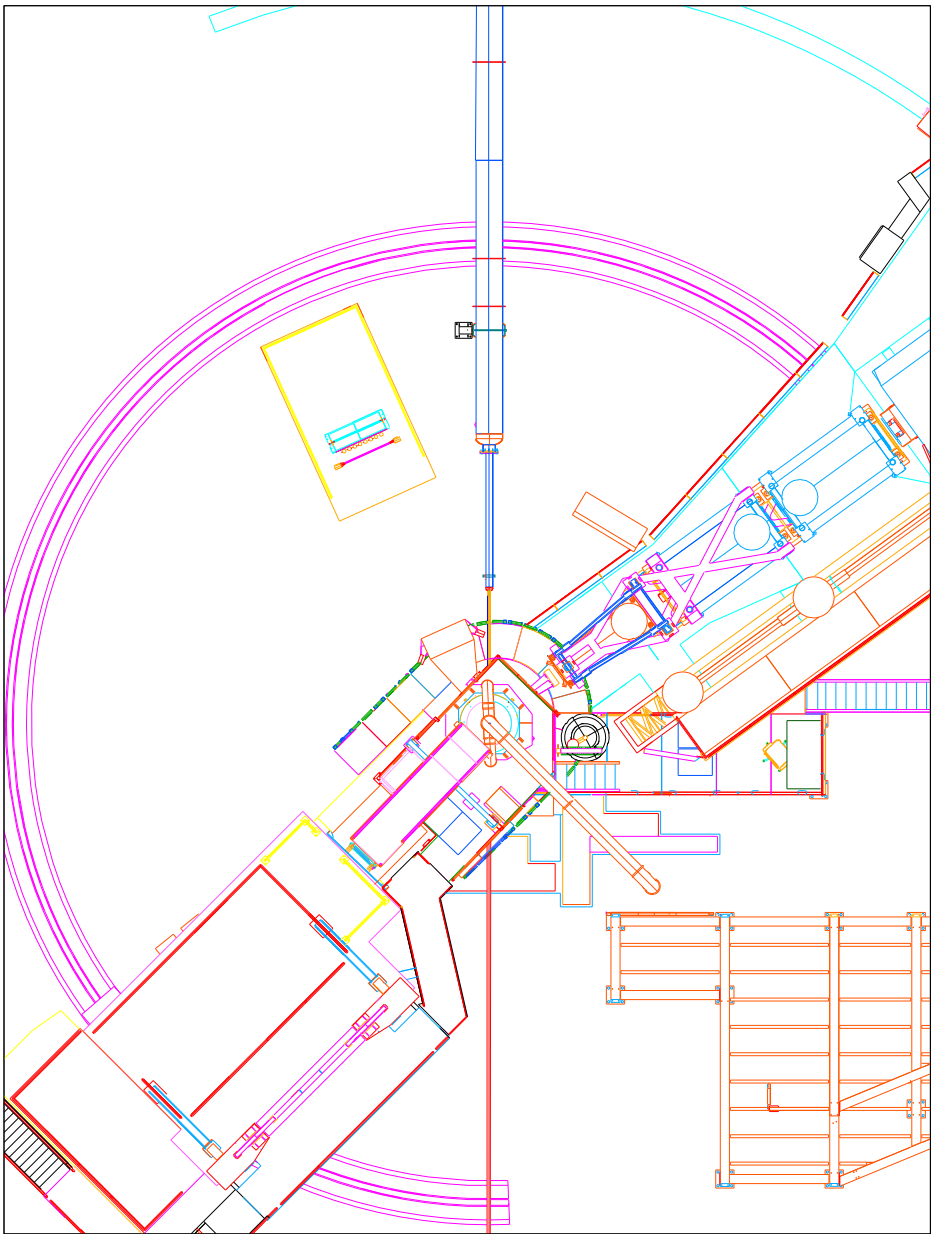

Figure 6: Kinematics for the proposed measurement. The $z^\star$ axis is defined by the $\vec{q}$ direction, the $y^\star$ axis is defined by $\vec{k} \times \vec{k'}$ with $\vec{k}$ and $\vec{k'}$ the momentum of the incident and the outgoing electrons, respectively. Target spin angles are shown for the case when the scattering plane is horizontal ($\phi^\star = 0°$).

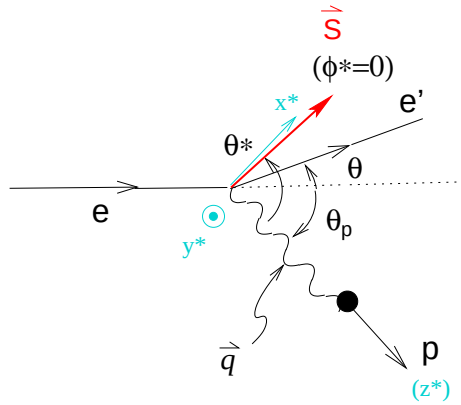

Figure 7: Hall C beam line chicane magnets and raster system. The BZ2 magnet and the beam-line downstream of the target will be replaced by a He bag.

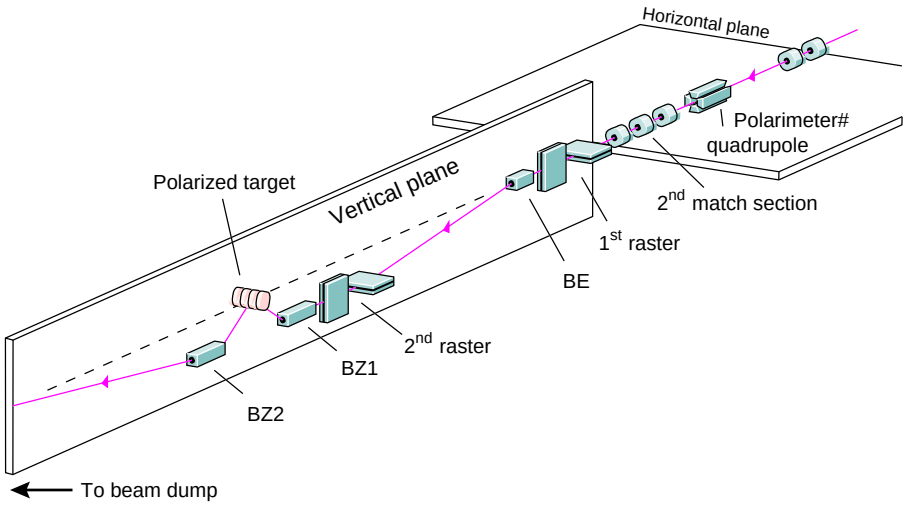

enters the target scattering chamber. A downstream chicane magnet will not be used. Instead a He bag will be used for transporting the beam downstream of the target to the beam dump. A series of chicane magnets were used for a similar purpose during the G_E^n experiment E93-026 [38] and the Resonance Spin Structure E01-006 [39], and we will use the same setup.

The beam needs to be rastered to maintain the target polarization and to ensure uniform distribution of both heat and radiation on the target material. We require the beam spot at the target to be ≈ 2 cm in

diameter which almost covers the entire target. This has been achieved during previous experiments [38, 39] using the slow rastering system. A schematic diagram for the beam-line chicane magnets and raster system is shown in Fig. 7.

Beam position monitoring and beam current measurement at our low current of 85 nA need special care. Using the same Secondary Emission Beam Position Monitor (SEM) [40] as in previous experiments E93-026 and E01-006, we believe a precise beam position monitoring can be achieved. An upgrade of the SEM electronics to operate in updating mode at the 30 Hz beam helicity flip rate is desirable, but not required. The beam current can be measured to a level of 5%. The effect of beam charge asymmetry will be discussed in Section 4.2.

3.3 The UVa NH_3 Target

We will use a solid polarized proton target developed by the University of Virginia (UVa). For the proposed measurement, the target material is $^{15}NH_3$. In this target, Dynamic Nuclear Polarization (DNP) is utilized to enhance the low temperature ($\approx$ 1 K), high magnetic field (5 T) polarization of solid materials. The irradiation of the target with 140 GHz microwaves drives hyperfine transitions which align the nucleon spins. This target was successfully used in the SLAC experiments E143, E155, E155x and two experiments E93-026 [38] and E01-006 [39] in Hall C. The proton polarization in $^{15}NH_3$ can reach as high as 95% and will decrease because of beam induced radiation damage. An average polarization of 75% was routinely achieved during previous experiments.

The target consists of a superconducting Helmholtz coils pair which operates at 5 Tesla, a ^{4}He evaporation refrigerator, a large pumping system, a high power microwave tube operating at frequencies around 140 GHz and an NMR system for measuring the target polarization. Figure 8 shows a slice through the target.

The target spin needs to be aligned at 41° and 80° w.r.t. the beamline for measurements of $Q^2 = 3.20$ and 5.60 (GeV/c)^2, respectively. Figure 9 shows the orientation of the target field and coils. For safety reasons, about 5 mm clearance is required between the raster outer edge and the coils.

The target cell is filled with frozen ammonia granules (1-2 mm in size), is fixed to a target holder stick (insert) and lowered into a cryostat of liquid ^{4}He. The nitrogen, helium and other target holder materials are in the acceptance of the spectrometers and will dilute the measured asymmetry. The thickness and density of each material are given in Table 1. The dilution factor will be discussed in Section 4.4. The packing factor is defined as the fraction of $^{15}NH_3$ to all materials in the target, and is usually measured using reference targets made of carbon disks (^{12}C) and ^{4}He. The unpaired proton in nitrogen can be polarized, hence a correction to the asymmetry must be made during analysis. The uncertainty due to the asymmetry from quasi-elastic scattering (QES) on nitrogen will be discussed in Section 4.5.

The target polarization needed is 75% (average) with 85 nA beam, measured by NMR to $\Delta P_t/P_t = 2.5\%$. During previous experiments, the NMR measurement was done continuously during the run. NMR readings were available every $\approx$ 20 seconds for on-line display, and were stored in special target event files for offline analysis. The price to pay for this is the presence of NMR pickup coils in the target cells, which should be accounted for in the dilution analysis. Figure 10 shows the geometry of the cell and the NMR coil used to measure proton polarization.

The radiation from the beam will lower the target polarization. This can be partially recovered by target annealing, a process where the $^{15}NH_3$ material is warmed from $\approx$ 1 K to $\approx$ 80 K. But eventually the target material needs to be changed for every 80 hours of 85 nA beam. We will use two cells per insert and at least one or possibly two insert changes will be needed during the experiment. Each insert change takes approximately 20 hours. The first $4 \sim 6$ hours and the $6 \sim 8$ hours at the end of an insert change are for thermal equilibrium (TE) calibrations and should be performed with the hall closed. In

Figure 8: Sideview of the UVa polarized NH_3 target.

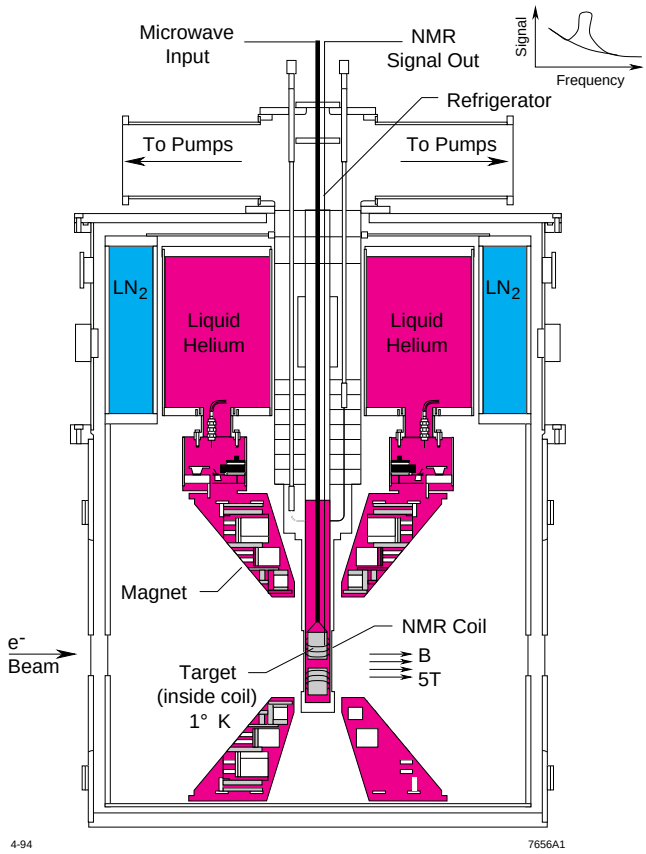

Table 1: Thickness and density for unpolarized materials along the beam-line.

Material	Thickness (cm)	Density (g/cm^3)
^{4}He (50% packing factor)	2.5	0.145
Al end-caps	0.00762	2.70
Copper in NMR coil	0.00673	8.96
Nickel in NMR coil	0.00289	8.75
Al windows in tail	0.00712	2.70
Al windows in LN_2 shield	0.00508	2.70
Al entrance window in cryostat†	0.00702	2.70
Al exit window in cryostat	0.01016	2.70

order to minimize the uncertainty of target polarization, we plan to perform additional TE calibrations opportunistically during the experiment.

Figure 9: Configuration of target coils for $Q^2 = 3.20$ (top) and 5.60 (bottom) measurements.

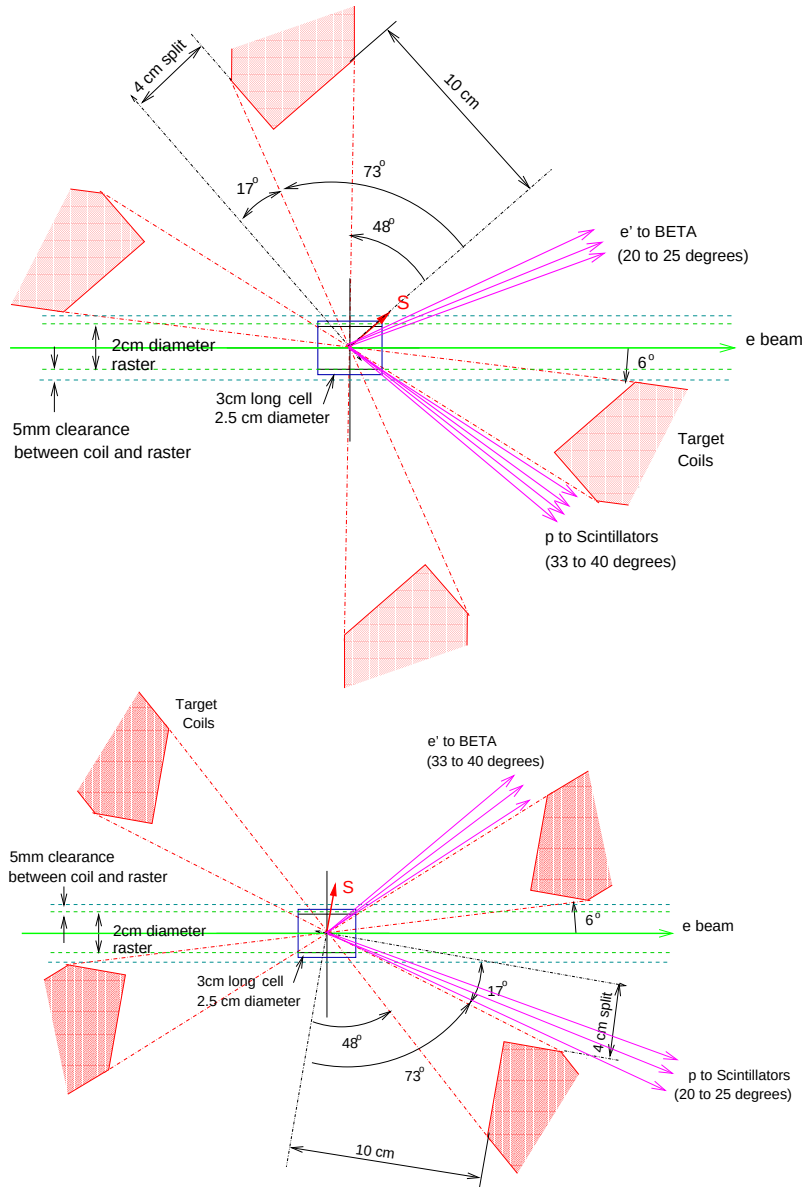

Figure 10: The 3-cm long by 2.5-cm diameter cylindrical target cell with the single loop coil used for measuring the proton polarization. Drawing not to scale.

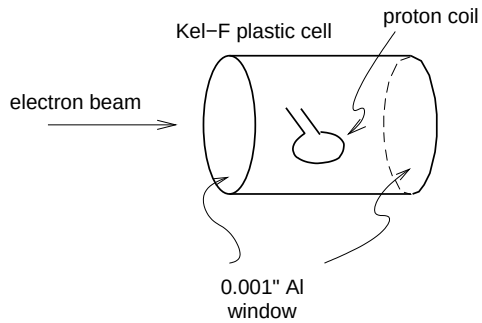

The strong magnetic field of the proposed target configuration will have an effect on the scattering charged particles but this can be well simulated. The uncertainty in the target spin direction will contribute to the systematic uncertainties of this experiment. During previous experiments the field direction has been measured to $0.1°$, and we require the same precision.

3.4 The BETA detector

For experiments using the polarized solid $^{15}\mathrm{NH}_3$ target, the luminosity is limited because of target depolarization due to beam heating. Hence a large acceptance detector system is highly desirable. For the proposed experiment, we will use the BETA (Big Electron Telescope Array) detector, currently being built for the SANE experiment [41], to detect scattered electrons. The basic structure of the BETA is shown in Fig. 11. It consists of a large electromagnetic calorimeter, a gas and a Lucite Čerenkov detector. The effective area of the BETA is 112cm(H)×232cm(V). Basic characteristics of the BETA is given in Table 2.

Table 2: Basic characteristics of the BETA detector.

Calorimeter Area	112 cm (H) $\times$ 232 cm (V)
Angular acceptance at 7 m	$\pm 4.6°$ (H), $\pm 9.5°$ (V)
Angle resolution at 7 m	1.5 mrad
Angular acceptance at 5 m	$\pm 6.4°$ (H), $\pm 13.3°$ (V)
Angle resolution at 5 m	2 mrad
Electron energy resolution	$5\%/\sqrt{E(\mathrm{GeV})}$

While the gas+Lucite Čerenkov hodoscope sector will be located at 83 cm away from the target as in the SANE experiment, the calorimeter sector of the BETA will be positioned at different distances for the two Q^2 measurements. For $Q^2 = 3.20$ (GeV/c)^2, the electron scattering angle is small so the calorimeter will be pulled back to 7 m away from the target to minimize the beam-line noise in the detector and to achieve a better resolution for electron's scattering angle. For $Q^2 = 5.60$ (GeV/c)^2, the total uncertainty in the asymmetry is dominated by statistics and the electrons have wider angular distribution than the

Figure 11: The BETA detector with its gas Čerenkov , Lucite Čerenkov , and calorimeter sections.

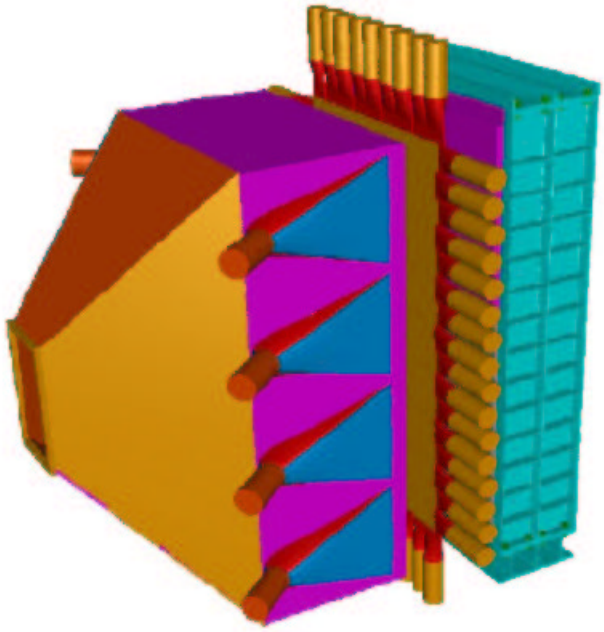

protons, we therefore place the calorimeter at 5 m away from the target to increase the counting rate while keeping a reasonable beam-line noise.

The BETA detector can be calibrated using the π^0 mass spectrum. This technique has been used in other experiments such as the RadPhi experiment (E94-016) [42] at CLAS and E852 at Brookhaven which employed a large calorimeter [43]. The gain monitoring system will be designed and constructed at UVa [44] for SANE based on the gain monitoring system that they successfully implemented for the RadPhi experiment.

The singles rates in the BETA detector have been calculated using a GEANT3-based simulation, as listed in Table 3. To estimate the effect of singles events on the measured asymmetries, we studied in the GEANT simulation the singles rate with analysis cuts in Q^2 and W applied. Figure 12 shows the W spectrum reconstructed from energy deposit in the calorimeter for electrons (black) and pions (red, green and blue). The pion yields in the figure are already suppressed by an off-line rejection factor of 1000 from the Čerenkov detector. Only a small fraction of singles electron events survive the Q^2 and W cuts, and the single pion rate is negligible within the W region of interest ($0.9 < W < 1.1$ GeV^2). The singles electron rate that will go into the final data analysis is no more than 1 Hz for $Q^2 = 3.20$ and 0.3 Hz for $Q^2 = 5.60$. In Section 4.6 we will discuss about the effect on the measured asymmetry caused by accidental coincidence events between the two detectors.

3.5 The Scintillator Array

In order to precisely measure the asymmetry of elastic events, it is necessary to suppress the quasi-elastic events and other background. This can be accomplished by detecting the protons simultaneously with the

Table 3: Singles rate (kHz) in the BETA detector. Čerenkov trigger rate is (Čerenkov e^+e^- rate + $\pi^+\pi^-$ rate $/100$ where 100 is the on-line Čerenkov pion rejection factor); Singles rate in the Calorimeter are given for 1 GeV threshold; Calorimeter trigger rate is the sum of e^+e^-, $\pi^+\pi^-$ and $\pi^0 pn$ rates; "BETA True" is the true coincidence rate of Čerenkov and Calorimeter; "BETA Accd" is the accidental coincidence rate of Čerenkov and Calorimeter.

Q^2 (GeV/c)^2	Čerenkov			Calorimeter				BETA	
	e^+e^-	$\pi^+\pi^-$	trigger	e^+e^-	$\pi^+\pi^-$	$\pi^0 pn$	trigger	True	Accd
3.20	0.30	166.03	1.96	0.27	0.99	12.70	13.97	0.28	0.01
5.60	0.60	210.72	2.71	0.07	0.22	3.47	3.77	0.08	0.00

Figure 12: Reconstructed W spectrum from the BETA for e^- (black), π^0 (red), π^+ (green) and π^- (blue). Vertical axis is in arbitrary unit. A Q^2 cut $|Q^2 - 3.2| < 0.5$ (GeV/c)^{2}was used in this figure. The pion yields are already suppressed by an off-line rejection factor of 1000 from the Čerenkov detector.

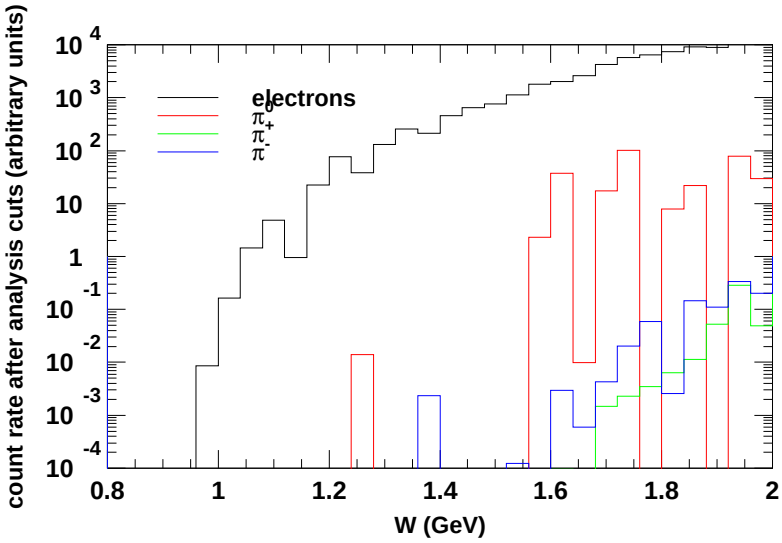

electrons and identifying elastic events by co-planarity conditions. For the proposed measurement we plan to use a scintillator array (SC) which consists three planes – one veto plane made by 15 11 cm$\times 1/4'' \times$ 160 cm thin scintillators (paddles), and two planes made by 16 10 cm$\times$10 cm $\times$160 cm thick scintillators (bars). The bars in the first plane will be oriented horizontally and those in the second plane will be arranged vertically. All scintillators will be provided by the UVa group of the collaboration. The thick bars are currently being used for the large neutron detector array for the Hall A G_E^n experiment E02-013 [45].

While protons deposit energy in the scintillators via minimal ionization, neutral particles lose energy via hadronic processes and give much smaller energy deposit. Therefore by using the energy deposit in

the thin veto plane, one can separate protons from neutrons and other neutral particles. In a 20-cm thick plastic (the two thick planes), most of $1-2$ (GeV/c) protons deposit > 30 MeV energy, which makes it possible to suppress the background in the SC by applying a high threshold (20-25 MeV). A 1-cm thick sheet of lead will be placed in front of the scintillator array to shield the low energy particles. The electronics can be borrowed from the Hall A collaboration. A movable stand to hold the scintillator array and the lead shield exists (Hall C). Small modifications to the stand will be needed to put the scintillator array above the horizontal plane.

A GEANT3-based simulation was performed to estimate the proton detection efficiency of the SC. With a 0.8 MeV threshold on the vetoes and a 35 MeV threshold on the bars, the probability of detecting a proton with signals that exceed these thresholds is 98.6% for protons in the 2-3 GeV/c range aimed straight at the center of the detector.

The singles rates in the SC were calculated in the same GEANT3-based simulation. The results are given in Table 4. We have also estimated the singles rate based on the test-run results performed for the approved high Q^2 G_E^n experiment E02-013 in Hall A [46]. In that test-run, a neutron detector prototype made of 4(width)$\times$5(depth) 10cm$\times$10cm$\times$160cm bars (thick bars) was placed at 25° and 8.3 m away from the target; there were 2" lead shield and two veto planes in front of the thick bar planes; iron converters were used both in front of the veto planes and between the thick bar planes to increase the energy deposit in the bars. The prototype was enclosed by a 1"-thick stainless steel box. The beam energy was 3.028 GeV and the current was 5 μA. The target was 50 mg/cm^2 BeO plus 700 mg/cm^2 ^{12}C (or 0.0172 radiation length total). The singles rate from the whole prototype was 150 KHz with a 40 MeVee threshold applied to the sum of 5 layers of bars, as shown in Fig. 13. No cut was applied on the veto signal. We will use this number for our singles rate estimation because applying a 40 MeV threshold on the energy deposit in 5 layers of bars is roughly equivalent to applying a 20 MeV threshold on 2 layers of bars. We scale this rate by the ratio of the target thickness (1.6 g/cm^2 for the NH_3 target), the ratio of the beam current 85 nA/5 μA, the front area of the detector 16 bars/4 bars, and the square of one over the drift distance from the target. Also take into account the fact that the NH_3 target field will increase the background by a factor of $2-3$ (3 will be used in the following); and assume that the angular dependence of the rate follows the Mott cross section, of which the $1/\sin^4(\theta/2)$ dependence adds another factor of 2 than a uniform distribution. We obtain ≈ 300 KHz for the total singles rate in our entire detector for the $Q^2 = 5.60$ (GeV/c)^2 kinematics, of which up to 70% comes from the vertically oriented bar closest to the beamline. We did not correct for the beam energy but this will not effect the estimate much because most of particles deposit energy in the scintillators through minimal ionization. Note that all the background suppression strategies, including lead shield between the detector and the beamline, and the stainless steel box used during the G_E^n test-run, can be used for the proposed measurement. Not all of them were not used in the GEANT3 simulation, which may explains why the estimate based on the G_E^n test-run results is lower than that from the GEANT3 simulation. It should also be mentioned that we keep standing on the safe side in the procedure described above, furthermore we did not correct for the iron converters used in the test-run, which can only give a higher estimate for the rate, so this result should provide a rather conservative estimate for the real singles rate in the SC if all the shieldings are implemented.

Overall, we estimate that in the worst case, the singles rate is < 500 KHz from the whole detector, and < 350 KHz from a single bar, which is not too high to handle.

For the proposed measurement, the triggering will be provided by the BETA. Each trigger will open a 60 ns window to collect signals from the SC. At a singles rate of 500 KHz, signal pileup in the SC might effect the measured asymmetry. At 500 KHz, the chance of having another particle in a 60 ns windows after the first event is 3%. Since the scintillator is segmented vertically, the average pileup possibility of a single scintillator bar is 0.2%. The uncertainty in the measured asymmetry due to pileup in the scintillators will be discussed in Section 4.8.

Table 4: Singles rate (kHz) in the Scintillator array. Thresholds for the veto and the bars trigger rates are 0.8 MeV and 20 MeV, respectively.

Q^2 (GeV/c)^2	Raw			Veto	Bars	Both
	e^+e^-	$\pi^+\pi^-$	π^0pn	trigger	trigger	trigger
3.20	0.64	244.41	866.38	801.54	761.98	688.67
5.60	0.57	277.95	945.05	964.48	924.23	844.92

3.6 Acceptance Matching and the Effect of the Target

The target has two effects on the scintillator and the BETA detector: Firstly, the large Helmholtz coils will block scattered particles and reduce the effective acceptance to about half of the naive value. Secondly, the target 5 T field will bend scattered particles slightly. This will cause a tilt of the scattering plane. The direct effects are that the target spin azimuthal angle $\phi^\star \neq 0$. For the proposed kinematics, the bending angle for electrons are 1.0° and 3.6° (bent down, towards the floor) and for protons are 4.8° and 3.48° (bent up, towards the ceiling), for $Q^2 = 3.20$ and 5.60 (GeV/c)^2, respectively. Figure 14 shows elastic event distribution in the two detectors. To center the tilted scattering plane at the center of BETA, the BETA needs to be lowered by 12 cm (31 cm) for $Q^2 = 3.20$ (5.60) (GeV/c)^2. Consequently, to match the angular acceptance of BETA, the scintillator array will be placed higher than the horizontal plane by 42 cm (30.5 cm) for $Q^2 = 3.20$ (5.60) (GeV/c)^2.

Figure 13: Test-run results for the singles rate of a neutron detector prototype. The test-run was performed in Hall A for the approved experiment E02-013. See text for details of the test-run conditions.

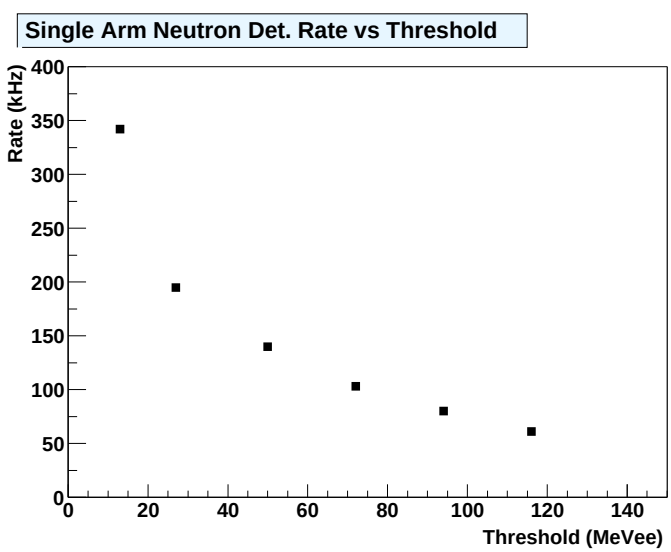

Figure 14: Angular distribution of elastic scattering events in the BETA (left) and the scintillator array (right) for $Q^2 = 3.20$ (top) and 5.60 (GeV/c)^2 (bottom). The BETA will be lowered by 12 cm (31 cm) for $Q^2 = 3.20$ (5.60) (GeV/c)^2, which corresponds to an out-of-plane angle of $1.0°$ ($3.6°$). The scintillator array will be placed higher than the horizontal plane by 42 cm (30.5 cm) for $Q^2 = 3.20$ (5.60) (GeV/c)^2, corresponding to an out-of-plane angle of $4.8°$ ($3.5°$). The boundaries of two detectors' acceptance are shown by red lines. Dashed lines show the center of the detectors.

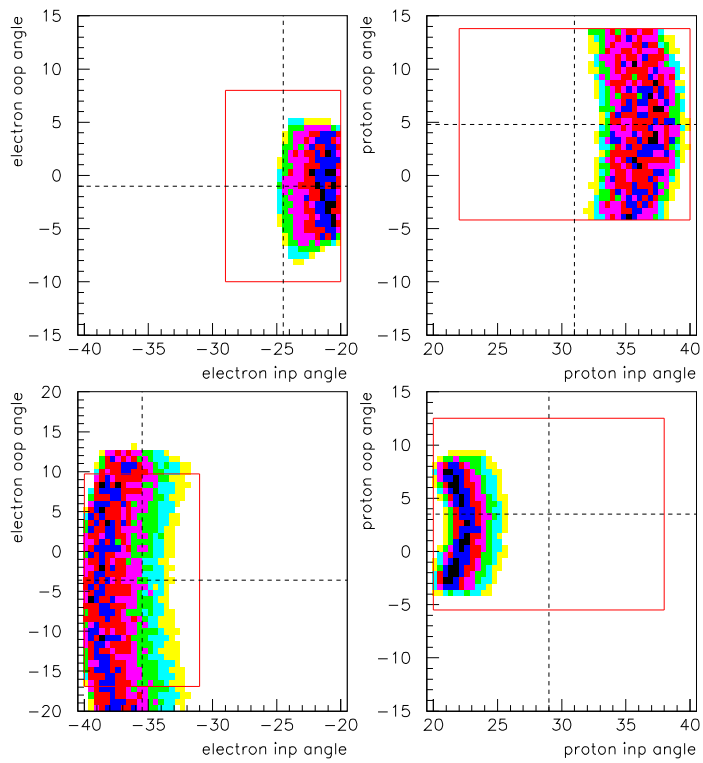

3.7 Data Analysis

The physics asymmetries can be extracted from the raw asymmetries as

$$A = \frac{A_{raw}(1-\eta_{A_N})}{P_{beam}P_{targ}f} \tag{1}$$

where $P_{beam} = 75\%$ and $P_{targ} = 75\%$ are the beam and target polarizations, f is the target dilution factor and η_{A_N} is a correction factor due to the asymmetry of quasi-elastic scattering electrons from the nitrogen in $^{15}NH_3$ (see Section 4.5 for the uncertainty of this correction).

The error in the asymmetry A is

$$\Delta A = \left\{ \left(\frac{\Delta A_{raw}}{f P_b P_t}\right)^2 + A^2\left[(\frac{\Delta P_b}{P_b})^2 + (\frac{\Delta P_t}{P_t})^2 + (\frac{\Delta f}{f})^2\right]\right\}^{1/2}, \tag{2}$$

$$\text{with} \qquad \Delta A_{raw} = \frac{1}{\sqrt{N}}, \tag{3}$$

where N is total number of events. The ratio G_E^p/G_M^p is extracted using Eq. (16) and its uncertainty from Eq. (17) of Appendix A. Detailed formulas for the error propagation from other error sources are given in Appendices A and B.

4 Expected Uncertainties and Rate Estimation

In this section we first list all uncertainty sources. Then we calculate the rate, the expected total uncertainties on $\mu G_E^p/G_M^p$ and the beam time.

4.1 Experimental Systematics

We estimate the uncertainty in the beam polarization to be 1.5% and the target polarization has 2.5% uncertainty. Other error sources include those from the target spin angle, beam energy $\Delta E/E = 2 \times 10^{-4}$ [37], BETA momentum resolution $\Delta E'/E' = 5\%/\sqrt{E'[\text{in GeV}]}$ and angle resolution $\Delta\theta = 0.3$ mrad [41]. Formula for error propagation from these experimental systematics to $\mu G_E^p/G_M^p$ are given in Appendix B. The largest systematic uncertainty comes from the error in the measurement of the target polarization.

4.2 Beam Charge Asymmetry

The beam charge is measured by the beam current monitor (BCM). The overall uncertainty in the BCM is about 5%. However the uncertainty in the beam charge asymmetry is expected to be much smaller than this value. In Ref. [47], the uncertainty on the beam charge asymmetry comes from (1) 1% from calibration offset; (2) 50 ppm from noise in the BCM signal; (3) 0.5% from the stability of the offset; and (4) $\approx$ 10 ppm from non-linearity for 85 nA current. The uncertainty on $\mu G_E^p/G_M^p$ due to beam charge asymmetry is about half of the error due to the target polarization (the latter is the dominant term of systematic uncertainties).

4.3 Target Polarization

Target polarization can be measured to 2.5% using NMR, as mentioned in Section 3.3. To minimize the uncertainty on the target polarization, we will perform additional thermal equilibrium (TE) calibration(s) opportunistically during the experiment, *i.e.* everytime when the beam is expected to be down for more than 6 hours. TE calibration should be performed with the hall closed.

4.4 Target Dilution Factor

The dilution factor is due to the quasi-elastic (QE) events from nitrogen in NH_3 and from other material listed in Table 1. A cut in the reconstructed invariant mass W will be used to select elastic events. Coplanary conditions will be used to suppress QE events – the measured energy and angle of scattered electrons will be used to calculate the proton scattering angle; then the results will be compared with the proton angle measured by the scintillator array. Figure 15 shows the difference between expected and measured proton scattering angles, for elastic events (red) and QE events (blue), and for both horizontal (in-plane) and vertical (out-of-plane) components. Cuts in the proton angle in both directions will be used in the analysis.

Figure 16 shows W spectra for simulated elastic events (red) and quasi-elastic events (green) for 1 mC beam charge. The dilution factor is defined as

Figure 15: Expected spectra on the scattered proton's in-plane angle $\delta\theta_{P,inp} \equiv \theta_{P,inp,detected} - \theta_{P,inp,el}$ and out-of-plane angle $\delta\theta_{P,oop} \equiv \theta_{P,oop,detected} - \theta_{P,oop,el}$ for the proposed measurements at $Q^2 = 3.20$ (left) and 5.60 (GeV/c)^2 (right). The red is for elastic, the black is for a Gaussian fit to the elastic peak, and the blue is for quasi-elastic events. A cut $0.8 < W < 1.2$ (GeV) was applied. Cuts $|\delta\theta_{P,inp}| < 0.044$ and $|\delta\theta_{P,oop}| < 0.044$ will be used to suppress the quasi-elastic events.

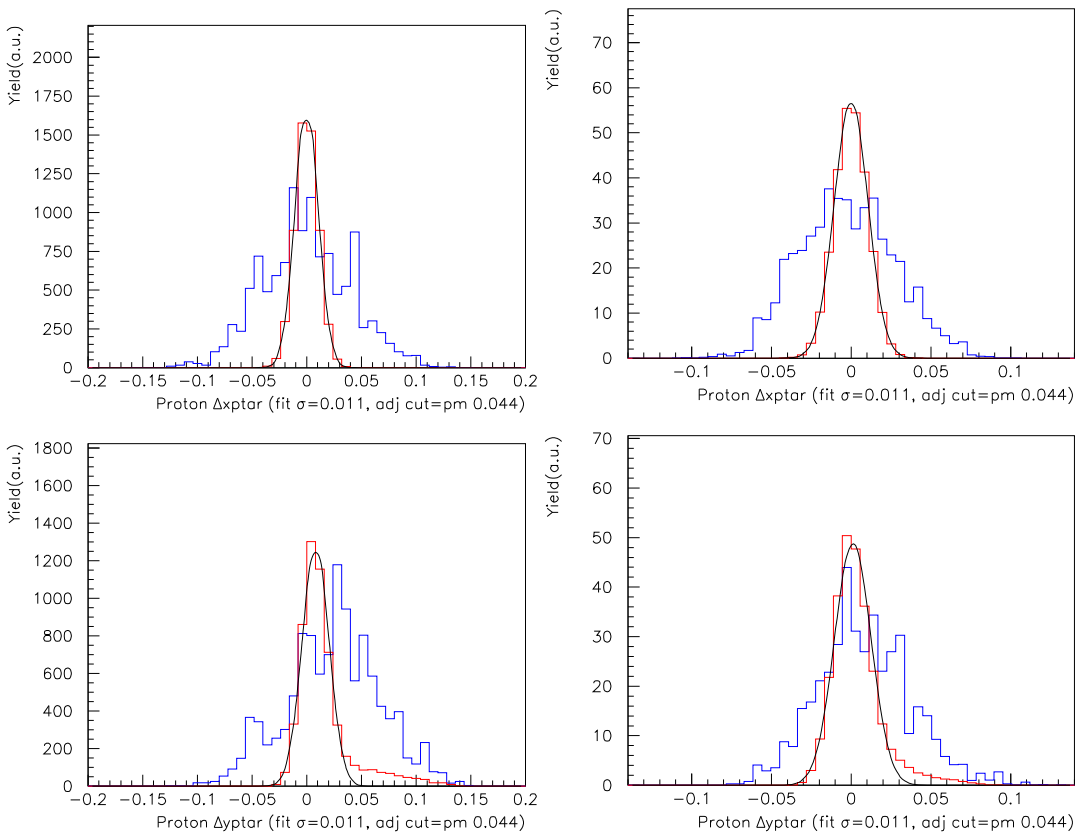

$$f = \frac{N_p}{N_p + N_{\mathrm{QE}}} \tag{4}$$

where N_p and N_{QE} are, respectively, yield of $e-p$ elastic events and quasi-elastic events from ^{15}N and other target material. We use $f = 0.7$ as a conservative estimate for all three kinematics in the rate and uncertainty estimation.

We will take data on carbon disks and He with approximately the same geometry as the NH_3 cell to measure the quasi-elastic cross sections, from which the dilution factor can be calculated. In E01-006 [39], the dilution factor is expected to be determined to an accuracy of $(2.5-3)\%$ over the final state invariant mass range $0.9 \leqslant W \leqslant 1.0$ GeV. We expect to achieve a 2.5% uncertainty at the elastic peak.

Figure 16: Expected invariant mass W spectra for the proposed measurements at $Q^2 = 3.20$ (top) and 5.60 (GeV/c)^2 (bottom). Simulations were performed using SIMC with subroutines specially written for the BETA and the scintillator array. Quasi-elastic events from ^{15}N and ^{4}He were simulated using the ^{12}C spectral function in the independent particle shell model (IPSM) and all other material were using the ^{56}Fe IPSM spectral function. The red shows the distribution for elastic events and the green for quasi-elastic events. Black lines show W-cuts used to estimate elastic rate and dilution factor f.

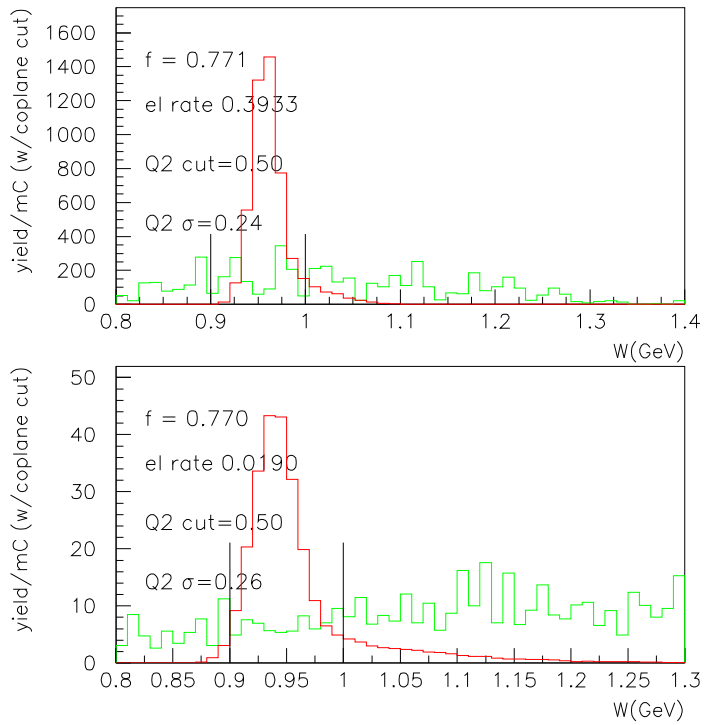

4.5 Nitrogen Asymmetry

The nitrogen in $^{15}NH_3$ is polarized and will contribute to the asymmetry. In the shell model, the ^{15}N nucleus has one unpaired proton which can be polarized. The polarization of the unpaired proton in ^{15}N is reduced from that of a free proton by several factors. First, the nitrogen in ^{15}N is polarized up to only $1/6$ of the proton, based on the Equal Spin Temperature (EST) hypothesis. Figure 17 shows data from Paul Scherrer Institute (PSI) in Switzerland and from SLAC experiments E143 and E155x, compared with EST predictions. Secondly, the proton in a polarized ^{15}N is only polarized to a certain amount. This quantity, called the effective nucleon polarization, has been estimated in two ways. In a model independent method [48, 49], $P_{p/^{15}\mathrm{N}} \approx -0.22$ based on isospin symmetry and data from beta decay of the mirror nucleus ^{15}O. In the shell model, the proton in ^{15}N is aligned anti-parallel to the nuclear spin $1/3$ of the time, hence $P_{p/^{15}\mathrm{N}} = -0.33$. Overall, the polarization of the unpaired proton is at most $(0.22 \sim 0.33) \times 1/6 P_p = 0.037 \sim 0.055 P_p$. In addition, only about $1/15$ of ^{15}N quasi-elastic (QE) events are from the $p_{1/2}$ proton, and not all the QE events are from the ^{15}N. The fraction of ^{15}N to total QE events is about $2/3$, which can be calculated from the packing factor measured using carbon disks

Figure 17: Polarization of nitrogen P_N in $^{15}NH_3$ *vs.* proton polarization P_p measured at PSI and during SLAC experiments E143 and E155x. The solid curve represents the prediction in the Equal Spin Temperature (EST) hypothesis and the dashed curve is a fit to world data.

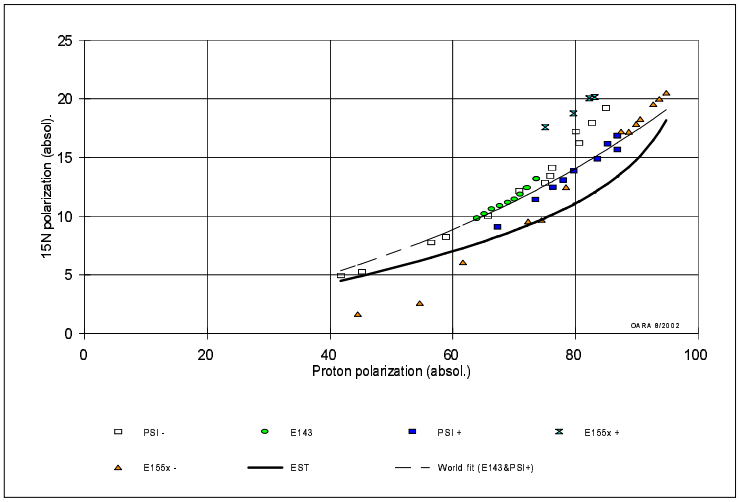

and ^{4}He as in E01-006 [39]. Also, there are three protons in $^{15}NH_3$. The correction to the measured asymmetry A_m due to nitrogen is therefore

$$A_m = fA_p + \frac{1}{3}\frac{2}{3}\frac{(1-f)}{15}A_{p/^{15}\mathrm{N}} = fA_p\Big(1 + (0.00054 \sim 0.00082)\frac{1-f}{f}\Big) \quad (5)$$

$$A_p = \frac{A_m}{f}\Big(1 - (0.00030 \pm 0.00006)\Big) \quad \text{if } f = 0.7 \quad (6)$$

Compared to the usually used $A = \frac{A_m}{f}$, we need to apply a 0.030% correction with $\pm 0.006\%$ uncertainty for both Q^2 points.

4.6 Background

For our measurement the main background comes from the quasi-elastic scattering from nitrogen and materials on the beam path. This part was discussed in the last section. Here we discuss about the effect from accidental coincidence events between the two detectors. In Section 3.4 we gave the singles rate of electrons and pions and estimated the rate that would pass analysis cuts in Q^2 and W. We found that at most $1(0.3)$ Hz of accidental electrons will survive the Q^2 and the W cuts at $Q^2 = 3.20(5.60)$ (GeV/c)^2. In Section 3.5 we gave the singles rate in the scintillator array (SC). From Fig. 15 the reconstructed proton angles (inp and oop) have a full width of $\approx$ 0.05 rad, which corresponds to $\approx$ 5$\times$ bar width (in vertical direction), or $\approx$ 5$\times$ timing resolution of one bar (in horizontal direction). Therefore by using co-planarity conditions we have a rejection factor of $\approx$ 3(v)$\times$3(h)= 9 for the singles events in the SC. With a coincidence timing window of 5 ns for offline analysis, the accidental coincidence rate is 1MHz$\times$5ns$\times$1Hz/9= 0.00055 and 1MHz$\times$6ns$\times$0.3Hz$/9$ = 0.0002Hz. Compared with the elastic rate 0.394 and 0.019 Hz in Table 5, and assuming that the asymmetry of the background is zero, the

accidentals will cause an extra $\leqslant 1\%$ dilution effect to the measured asymmetry. To make sure that the data from carbon disks and He have the same dilution effect from accidentals as the polarized target runs, the carbon and He runs should be taken with the same luminosity as the NH_3 runs.

4.7 Electromagnetic Radiative Corrections

We discuss here electromagnetic radiative corrections besides possible large corrections from the two-photon exchange process. The "traditional" radiative corrections can be calculated using Mo and Tsai's formalism [20] and the uncertainty of the correction to elastic asymmetries is negligible.

4.8 Deadtime Correction

The total coincidence rate of our proposed measurement is very low, a few tens of Hz, hence the electronic dead time comes mainly from events pileup in the scintillators (SC). In Section 3.5 we showed that the possibility to have two-events pileup in the scintillators (SC) is about 0.2%. Assuming there is 1% difference in the SC singles rate between two beam helicity states, the pileup will cause a 0.2% relative loss and a $0.2\% \times 1\%/2 = 10$ ppm offset to the measured asymmetry. To study the 0.2% correction to the asymmetry, we plan to do a few hours' rate studies during commissioning, perform measurement from 60 nA to about 120 nA, and extrapolate to zero rate. Here the minimum current is limited by what the MCC can control and the maximum current is determined by how much the target can take. The angular dependence of the deadtime will also be studied and taken into account in the analysis Computer deadtime can be measured by triggers and the uncertainty is determined by the statistics of each run. We require a run to have at least 1M events. Overall, a conservative estimate for the uncertainty in the asymmetry due to deadtime correction is no larger than 0.2%.

4.9 Optimization of Kinematics

We optimize the kinematics based on the following conditions:

- For a given Q^2, the rate is maximized by varying beam energy and scattering angle;
- For given Q^2 and beam energy, the total uncertainty of $\mu G_E^p/G_M^p$ is minimized by varying target spin angle;
- Target coils do not interfere with either beam-line or the central trajectories of scattered electrons and protons. A 0.5 cm clearance is required between coils and the outer edge of the beam. Loss in the acceptance due to possible partial blocking of the scattered particles' trajectory is estimated in the simulation.

Results are shown in Fig. 18 and 19. We choose to use a 5.552 GeV beam. Target spin will be pointing to the left and aligned at 41° and 80° *w.r.t* the beam-line.

4.10 Summary of Rate and Expected Uncertainties

We use the Bosted fit [51] for G_M^p and G_E^p to calculate the elastic $e-p$ cross section. Using a 3 cm target cell and 85 nA beam current the luminosity available is 8.5×10^{34} cm^2/s. The expected results are shown in Fig. 20. Kinematics, rates and expected uncertainties for the proposed measurements are given in Table 5, where

Figure 18: Expected total uncertainties of $\mu G_E^p/G_M^p$ *vs.* target spin angle for $E = 5.552$ GeV and fixed beam time, 119.5 and 254.1 hours for $Q^2 = 3.20$ and 5.60 (GeV/c)^2, respectively. Here negative spin angle means the target spin is pointing to the left of beam-line. Red/blue/green boxes show the interference between coils and beam-line/ scattered electrons/ scattered protons. Red stars show the selected kinematics.

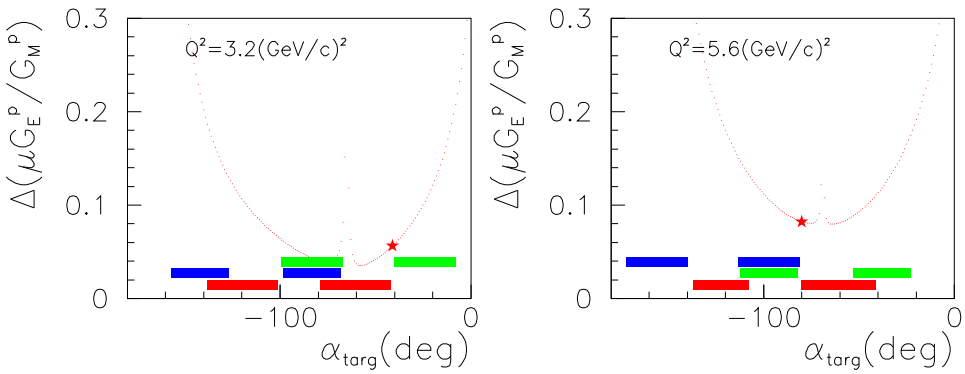

Figure 19: Expected total uncertainties of $\mu G_E^p/G_M^p$ *vs.* beam energy for fixed beam time, 119.5 and 254.1 hours for $Q^2 = 3.20$ and 5.60 (GeV/c)^2, respectively. Red stars show the beam energy needed by the proposed measurement.

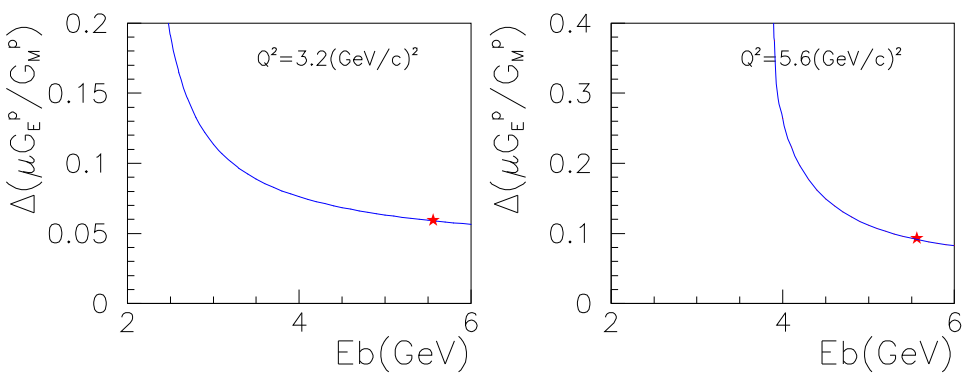

◇ E is beam energy;

◇ θ_e and E' are the nominal angle and momentum of scattered electrons of the Q^2 range of interest;

◇ θ_p and p_p are the nominal angle and momentum of scattered protons; only the angle will be detected.

◇ $\theta^\star$ and $\phi^\star$ are the polar and azimuthal angles of target spin;

◇ A_{el} and $A_{el,bosted}$ are elastic asymmetries calculated from Hall A polarization transfer (PT) fit and Bosted fit, respectively;

◇ A_{raw} is expected measured asymmetry using PT fit;

◇ N_{tot} is total number of events under the elastic peak, $N_{tot} = N_{el,tot}/f$;

◇ Systematic uncertainty on asymmetries including 1.5% from beam polarization, 2.5% from target

polarization, 2.5% from target dilution factor, $\approx 1.2\%$ from charge asymmetry, 0.35% from QE events from nitrogen, and 0.2% from deadtime correction.

◇ rates from simulation take into account the loss in acceptance due to target coil blocking.

◇ coplanary conditions were included in the rate and dilution estimation.

Table 5: Kinematics, rate and expected uncertainties for the proposed measurements.

Q^2 (GeV/c)^2	3.20	5.60
E (GeV)	5.552	5.552
θ_e	22.32°	36.53°
E' (GeV)	3.847	2.568
θ_p	36.24°	23.66°
p_p (GeV/c)	2.471	3.809
$\theta^\star$	77.24°	103.66°
$\phi^\star$	0.60°	1.47°
A_{el}	-0.202	0.129
A_{raw}	-0.0797	0.0508
$(A_{el,bosted} - A_{el})/A_{el}$	24.88%	-125.06%
σ (nb/sr)	0.451	0.009
elastic rate (simulation, Hz)	0.394	0.019
total rate (el rate/f, Hz)	0.563	0.027
N_{tot}	242K	25K
Uncertainty on asymmetries		
Statistical	2.548%	12.463%
Systematic	3.418%	3.418%
Total	4.263%	12.923%
Uncertainty on $\mu G_E^p/G_M^p$		
$\Delta P_{beam}/P_{beam} = 1.5\%$	0.0219	0.0102
$\Delta P_{targ}/P_{targ} = 2.5\%$	0.0292	0.0135
Target dilution $\Delta f/f = 2.5\%$	0.0292	0.0135
Beam charge asymmetry	0.0163	0.0087
Nitrogen asymmetry	0.0000	0.0000
Deadtime correction	0.0029	0.0014
$\Delta E/E = 5 \times 10^{-4}$	0.0001	0.0004
$\Delta E'/E' = 5\%/\sqrt{E'(GeV)}$	0.0102	0.0444
$\Delta\theta_e = 2.2$ mrad (7m)	0.0058	
$\Delta\theta_e = 3$ mrad (5m)		0.0118
Target spin orientation (inp) 0.1°	0.0025	0.0068
Target spin orientation (oop) 0.1°	0.0000	0.0000
Total syst.	0.0510	0.0520
Total stat.	0.0372	0.0844
Beam time (hours)	119.5	254.1
Expected $\mu G_E^p/G_M^p$	0.589	0.277
Total uncertainty $\Delta(\mu G_E^p/G_M^p)$	± 0.063	± 0.099

Figure 20: Expected results and full uncertainties of the proposed measurements (red solid circles) along with world data. Curves are from the Bosted parameterization (solid) [51], a fit to the Hall A polarization transfer results (dashed) [13] and Arrington's global fit to the cross section data (dash-dotted) [15].

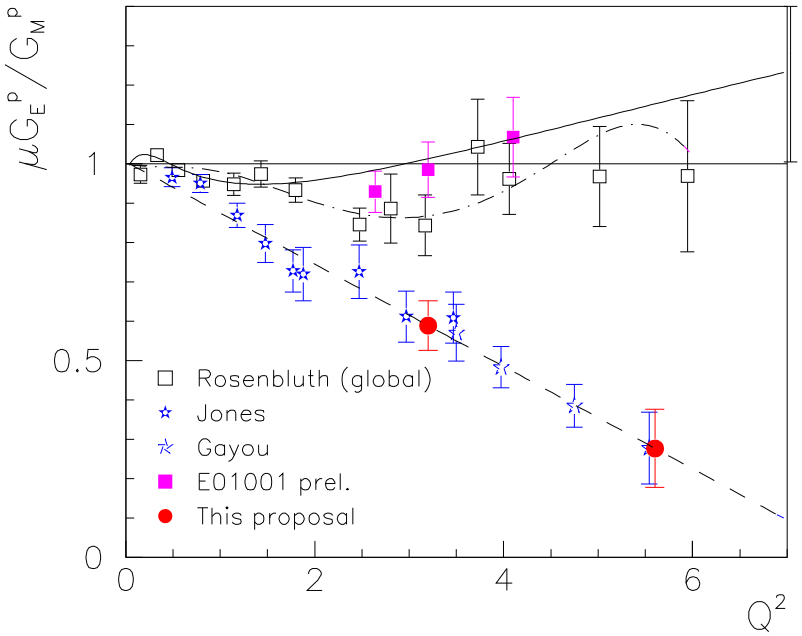

5 Beam Time Request

Our beam time request is given in Table 6. We ask for 17 PAC days for production data taking, target dilution factor measurement, Møller and arc measurements. We ask for 6 PAC days overhead time for one beam pass change and target work. If this experiment can run immediately before or after the approved E03-109 [41], then no additional time for target and the BETA installations will be needed.

Table 6: Detector settings, total beam time and overhead time for the proposed measurements.

Q^2 (GeV/c)^2	3.20	5.60
E (GeV)	5.552	5.552
BETA (calo) drift distance	7 m	5 m
BETA central inp angle	24.5°	35.5°
BETA central oop angle	−1.0° (−12 cm)	−3.6° (−31 cm)
SC drift distance	5 m	5 m
SC central inp angle	35°	29°
SC central oop angle	4.8° (42 cm)	3.5° (35 cm)
Production time	119.5	254.1
carbon and helium runs	6	12
Møller measurement	4	9
arc measurement	4	
Total beam time (PAC hours)	408	
BETA and SC coincidence commissioning	64	
BETA and SC configuration change	48	
Target field rotation†	24	
Target field survey	10	
Target anneal	78	
Two target insert changes	46	
Total overhead (clock hours)	240	

† target field rotation can be performed partly at the same time as BETA and SC configuration change

6 Comparison to PR04-014

The PAC-25 report [53] on PR04-014 is given in Appendix C. While the physics motivation of the proposed measurement remains the same, the experimental setup has been changed completely. With the new coincidence setup of two large acceptance detectors, the Q^2 range proposed here is significantly higher than that in PR04-014.

7 Summary

We propose to make measurements of G_E^p/G_M^p via the asymmetry in doubly polarized elastic $\vec{p}(\vec{e}, e'p)$ scattering at $Q^2 = 3.20$ and 5.60 (GeV/c)^2. Assuming 75% beam polarization and 85 nA current, we request 17 days of beam time and 6 days overhead. The proposed measurement will provide the first data for G_E^p/G_M^p from the $\vec{p}(\vec{e}, e')p$ asymmetry method in intermediate Q^2 range with good precision. This

new method is expected to be less sensitive to two-photon exchange contributions than the Rosenbluth separation technique, and it does not suffer from the same systematic uncertainties as previous polarization transfer measurements. These data will provide an important check on the polarization transfer results. When combined with the recent check on the Rosenbluth separation results, the new data will either confirm that two-photon exchange or other missing physics is a necessary ingredient in future calculations, or they will point to a possible systematic error in prior experimental techniques.

A Doubly Polarized Elastic Scattering

For elastic scattering the unpolarized cross section is given by

$$\left(\frac{\mathrm{d}^2\sigma}{\mathrm{d}\Omega \mathrm{d}E'}\right)^u = \sigma_M \frac{E'}{E}\left(\frac{G_E^2+\tau G_M^2}{1+\tau} + 2\tau G_M^2 \tan^2(\theta/2)\right), \tag{7}$$

where $Q^2 = 4EE'\sin^2(\theta/2)$, $\tau = Q^2/(4M^2)$, the energy of scattered electrons is $E' = E/\left[1+\frac{2E}{M}\sin^2(\theta/2)\right]$, M is the nucleon mass, E is the beam energy and θ is the electron scattering angle. The Mott cross section is

$$\sigma_M \equiv \left(\frac{\mathrm{d}\sigma}{\mathrm{d}\Omega}\right)_{Mott} = \frac{\alpha^2\cos^2\frac{\theta}{2}}{4E^2\sin^4\frac{\theta}{2}}. \tag{8}$$

The momentum and the angle of the scattered protons are

$$p_p = \sqrt{Q^2 + \left(\frac{Q^2}{2M}\right)^2} \text{ and} \tag{9}$$

$$\cos\theta_p = \frac{(M+E)\sqrt{M^2+p_p^2} - M^2 - ME}{p_p E}. \tag{10}$$

For the case of polarized electrons scattering off a polarized nucleon target, the cross section difference between opposite electron helicity states is given by [52]

$$\frac{1}{2}\left[\sigma^+ - \sigma^-\right] = -2\sigma_M \frac{E'}{E}\sqrt{\frac{\tau}{1+\tau}}\tan\frac{\theta}{2}\left\{\sqrt{\tau\left(1+(1+\tau)\tan^2\frac{\theta}{2}\right)}\cos\theta^\star G_M^2 + \sin\theta^\star\cos\phi^\star G_M G_E\right\}, \tag{11}$$

where the superscript $\pm$ denotes the helicity of the incident electrons, θ^* and ϕ^* are the polar and the azimuthal angles of the target spin direction as shown in Fig. 21. The asymmetry is

$$\begin{aligned} A &\equiv \frac{\sigma^+ - \sigma^-}{\sigma^+ + \sigma^-} \\ &= -\frac{2\sqrt{\frac{\tau}{1+\tau}}\tan\frac{\theta}{2}\left\{\sqrt{\tau\left(1+(1+\tau)\tan^2\frac{\theta}{2}\right)}\cos\theta^\star G_M^2 + \sin\theta^\star\cos\phi^\star G_M G_E\right\}}{\frac{G_E^2+\tau G_M^2}{1+\tau} + 2\tau G_M^2\tan^2(\theta/2)}, \end{aligned} \tag{12}$$

Equation (12) can be written as

Figure 21: Polar and azimuthal angles of the target spin. Here $\vec{S}$ is the target spin, $\vec{q}$ is the three momentum transfer. The $z^\star$ axis is defined by $\vec{q}$, $y^\star$ axis is defined by $\vec{k} \times \vec{k}'$ with $k(k')$ the three momentum of the incident and scattered electrons.

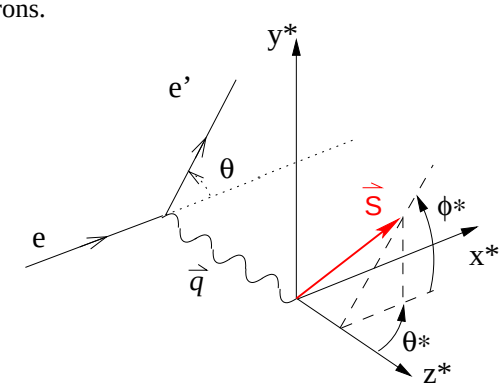

$$\left(\frac{G_E}{G_M}\right)^2 + B\left(\frac{G_E}{G_M}\right) + C \quad = \quad 0\,, \tag{13}$$

where

$$B \quad = \quad \frac{2}{A}\sqrt{\tau(1+\tau)}\tan\frac{\theta}{2}\sin\theta^\star\cos\phi^\star\,, \tag{14}$$

$$C \quad = \quad \tau + 2\tau(1+\tau)\tan^2\frac{\theta}{2} + \frac{2\cos\theta^\star}{A}\left\{\sqrt{\tau(1+\tau)}\tan\frac{\theta}{2}\sqrt{\tau\left[1+(1+\tau)\tan^2\frac{\theta}{2}\right]}\right\} \tag{15}$$

with A the measured elastic asymmetry. Therefore ratio G_E/G_M can be calculated as

$$\frac{G_E}{G_M} \quad = \quad \frac{1}{2}\left(-B \pm \sqrt{B^2-4C}\right)\,, \tag{16}$$

the sign is kinematic dependent. The uncertainty due to the error in asymmetry is given by

$$\Delta\left(\frac{G_E}{G_M}\right) \quad = \quad \frac{\Delta A}{2}\left|\left(\frac{\mathrm{d}B}{\mathrm{d}A}\right)\left(-1 \pm \frac{B}{\sqrt{B^2-4C}}\right) \pm \left(\frac{\mathrm{d}C}{\mathrm{d}A}\right)\frac{-2}{\sqrt{B^2-4C}}\right| \tag{17}$$

$$\text{where} \qquad \frac{\mathrm{d}B}{\mathrm{d}A} = -\frac{B}{A}$$

$$\text{and} \qquad \frac{\mathrm{d}C}{\mathrm{d}A} = -\frac{C - \left[\tau + 2\tau(1+\tau)\tan^2\frac{\theta}{2}\right]}{A}$$

B Error Propogation of Systematic Uncertainties for G_E^p/G_M^p

The uncertainty in G_E^p/G_M^p due to the uncertainty in asymmetry ΔA is given by Eq. (17) where ΔA is from Eq. (2). In this appendix we give experimental systematics due to uncertainties in E, E', θ, $\theta^\star$ and $\phi^\star$.

From Eq. (16) the uncertainty in G_E/G_M due to the uncertainty in E is given by

$$\Delta\left(\frac{G_E}{G_M}\right) \quad = \quad \frac{\Delta E}{2}\left|\left(\frac{\mathrm{d}B}{\mathrm{d}E}\right)\left(-1 \pm \frac{B}{\sqrt{B^2-4C}}\right) \pm \left(\frac{\mathrm{d}C}{\mathrm{d}E}\right)\frac{-2}{\sqrt{B^2-4C}}\right| \tag{18}$$

the same equation stands for E', θ, $\theta^\star$ and $\phi^\star$. For E we have

$$\frac{\mathrm{d}B}{\mathrm{d}E} = \frac{\partial B}{\partial \tau}\frac{\mathrm{d}\tau}{\mathrm{d}E}\ , \quad \frac{\mathrm{d}C}{\mathrm{d}E} = \frac{\partial C}{\partial \tau}\frac{\mathrm{d}\tau}{\mathrm{d}E} \tag{19}$$

where

$$\begin{aligned}
\frac{\partial B}{\partial \tau} &= \frac{1}{2}\big(\frac{B}{\tau} + \frac{B}{1+\tau}\big)\ , \\
\frac{\partial C}{\partial \tau} &= 1 + 2(1+\tau)\tan^2\frac{\theta}{2} + \frac{\tan\frac{\theta}{2}}{2A}\cos\theta^\star\Bigg\{2\sqrt{(1+\tau)\Big[1+(1+\tau)\tan^2\frac{\theta}{2}\Big]} \\
&\quad + \sqrt{\frac{1+(1+\tau)\tan^2\frac{\theta}{2}}{1+\tau}} + \tau\tan\frac{\theta}{2}\sqrt{\frac{1+\tau}{1+(1+\tau)\tan^2\frac{\theta}{2}}}\Bigg\} \\
\text{and}\ \frac{\mathrm{d}\tau}{\mathrm{d}E} &= \frac{\tau}{E}\ ,
\end{aligned} \tag{20}$$

For θ we have

$$\frac{\mathrm{d}B}{\mathrm{d}\theta} = \frac{\mathrm{d}B}{\mathrm{d}\theta} + \frac{\partial B}{\partial \tau}\frac{\mathrm{d}\tau}{\mathrm{d}\theta}\ , \quad \frac{\mathrm{d}C}{\mathrm{d}\theta} = \frac{\mathrm{d}C}{\mathrm{d}\theta} + \frac{\partial C}{\partial \tau}\frac{\mathrm{d}\tau}{\mathrm{d}\theta} \tag{21}$$

where

$$\frac{\mathrm{d}\tau}{\mathrm{d}\theta} = \frac{EE'}{2M^2}\sin\theta\ , \quad \frac{\mathrm{d}B}{\mathrm{d}\theta} = \frac{B}{\sin\theta}$$

For E' we have

$$\frac{\mathrm{d}B}{\mathrm{d}E'} = \frac{\partial B}{\partial \tau}\frac{\mathrm{d}\tau}{\mathrm{d}E'} + \frac{\mathrm{d}B}{\mathrm{d}\theta^\star}\frac{\mathrm{d}\theta^\star}{\mathrm{d}E'}\ , \quad \frac{\mathrm{d}C}{\mathrm{d}E'} = \frac{\partial C}{\partial \tau}\frac{\mathrm{d}\tau}{\mathrm{d}E'} + \frac{\mathrm{d}C}{\mathrm{d}\theta^\star}\frac{\mathrm{d}\theta^\star}{\mathrm{d}E'} \tag{22}$$

$$\text{where}\ \frac{\mathrm{d}\tau}{\mathrm{d}E'} = \frac{\tau}{E'}\ .$$

The target spin polar angle $\theta^\star$ is determined by the field orientation and the proton scattering angle. The target field direction can be measured to 0.1° and the uncertainty in the proton angle is determined by the electron momentum $\Delta E'/E'$ as

$$\frac{\mathrm{d}\theta^\star}{\mathrm{d}E'} = \frac{\mathrm{d}\theta_p}{\mathrm{d}E'} = \frac{(M+E)M}{\big(2M+\nu\big)^{3/2}E\sin\theta_p}\ . \tag{23}$$

C PAC-25 report for PR04-014

Individual Proposal Report

Proposal : PR 04-014

Scientific rating : N/A

Title : Measurement of G^p_E/G^p_M using elastic polarized reaction $e(p,e')p$ up to $Q^2 = 3.50$ $(GeV/c)^2$

Spokespersons : X. Zheng, J.R. Calarco and O.R. Rondon

Motivation: The determination of the proton EM form factors is of considerable physics interest, generating a wealth of experiments aiming at reaching the largest values of Q^2 possible. An experimental discrepancy has recently been observed between the results from the conventional Rosenbluth separation technique and those from a recoil polarization technique, when the two sets of results are interpreted in the absence of two-photon contributions. Initially the discrepancy raised experimental questions, and, as a consequence, the separation technique has been checked by a new analysis of the existing data and measurements performed at JLab. The discrepancy at large Q^2 has been attributed to the effect of two-photon exchange, which was neglected until recently, and theoretical calculations have accounted for part of the experimental deviation.

It is important to pin down the origin of the observed experimental discrepancy in order to allow the unambiguous extraction of the proton elastic form factors and to test the two-photon exchange calculations. This proposal is aiming at providing a new experimental observable. The measurement of the asymmetry in a doubly-polarized experiment should indeed provide an identical result to the transfer polarization data. This would then be a cross check, but with very different systematic errors.

Measurement and Feasibility: The experiment is proposed for Hall C and requests 25 days of running time. It is an asymmetry measurement using a polarized NH_3 target and a polarized electron beam of 6 GeV. This is a single-arm experiment, with the detection of the elastically scattered electron in HMS with its standard equipment. The electron beam intensity is limited to 85 nA by the polarized target. The spin orientation of the target and the scattered electrons detection angle are optimized in the angular regions allowed by the design of an existing polarized target. The asymmetry measurements, providing the ratio of the EM proton form factors, will be measured at two Q^2 values (2.1 and 3.5 $(GeV/c)^2$) with a measurement at lower Q^2 (3.6 GeV beam) to control the value of the product of the polarizations of the beam and target. The experiment appears feasible with the expected precision.

Issues: The PAC has, however, considered that given the present experimental situation a cross check of the transfer polarization data is not sufficient at the level of accuracy proposed. It has not been convinced that the range in Q^2 covered in the measurement is large enough nor that the precision it can attain makes a sufficiently compelling case for approval.

Recommendation : Defer

References

[1] F. Iachello, A.D. Jackson and A. Lande, Phys. Lett. B **43**, 191 (1973); E.L. Lomon, Phys. Rev. C **64**, 035204 (2001).

[2] S.J. Brodsky and G. Farrar, Phys. Rev. D **11**, 1309 (1975).

[3] S.J. Brodsky and G.P. Lepage, Phys. Rev. D **22**, 2157 (1981).

[4] P.L. Chung and F. Coester, Phys. Rev. D **44**, 229 (1991).

[5] M.R. Frank, B.K. Jennings and G.A. Miller, Phys. Rev. C **54**, 920 (1996).

[6] D.H. Lu, A.W. Thomas and A.G. Williams, Phys. Rev. C **57**, 2628 (1998).

[7] F. Cardarelli and S. Simula, Phys. Rev. C **62**, 065201 (2000); S. Simula, e-Print nucl-th/0105024.

[8] R.F. Wagenbrunn *et al.*, Phys. Lett. B **511**, 33 (2001); S. Boffi *et al.*, Eur. Phys. J. A **14**, 17 (2002).

[9] G.Holzwarth, Zeitschr. Fuer Physik A **356**, 339 (1996), e-Print hep-ph/9606336; e-Print hep-ph/0201138 and ref. therein.

[10] A.F. Sill *et al.*, Phys. Rev. D **48**, 29 (1993).

[11] J. Arrington, Phys. Rev. C **69**, 022201 (2004).

[12] M.K. Jones *et al.*, Phys. Rev. Lett. **84**, 1398 (2000).

[13] O. Gayou *et al.*, Phys. Rev. Lett., **88**, 092301 (2002).

[14] O. Gayou *et al.*, Phys. Rev. C **64**, 038202 (2003).

[15] H. Budd, A. Bodek and J. Arrington, to be published in Nucl. Phys. B, e-Print Archive: hep-ex/0308005.

[16] J. Arrington, Eur. Phys. J. **A17**, 311 (2003); Phys. Rev. C **68**, 034325 (2003).

[17] J. Arrington and R. Segel, JLab E01-001, New Measurement of (GE/GM) for the Proton. For preliminary results, see e-Print: nucl-ex/0312017.

[18] E. Brash, C. Perdrisat and V. Punjabi, JLab E01-109, Measurement of Gep/Gmp to Q2=9 GeV2 via Recoil Polarization.

[19] J. Mar *el al.* Phys. Rev. Lett. **21**, 482 (1968).

[20] L. Mo, Y.S. Tsai, Rev. Mod. Phys. **41**, 205 (1969).

[21] P.A.M. Guichon and M. Vanderhaeghen, Phys. Rev. Lett. **91**, 142303 (2003).

[22] P.G. Blunden, W. Melnitchouk and J.A. Tjon, Phys. Rev. Lett. **91**, 142304 (2003).

[23] M.P. Rekalo and E. Tomasi-Gustafsson, e-Print: nucl-th/0307066.

[24] Y.C. Chen, A. Afanasev, S.J. Brodsky, C.E. Carlson, M. Vanderhaeghen, SLAC-PUB-10366, JLAB-THY-04-10, WM-04-103, Mar 2004. 4pp. e-Print Archive: hep-ph/0403058

[25] A. Afanasev, *priv. comm.*

[26] M. Vanderhaegen, *priv. comm.*

[27] J. Arrington, Phys. Rev. C **69**, 032201 (2004).

[28] W. Brooks *et al.*, Beyond the Born Approximation: A Precise Comparison of e^+p and e^-p Elastic Scattering In CLAS, proposal to be submitted to JLab PAC-26.

[29] J. Arrington *et al.*, A Measurement of Two-Photon Exchange Contribution in ep Elastic Sccatering, proposal to PAC-25.

[30] A. De Rujula, J.M. Kaplan, and E. De Rafael, Nucl. Phys. B **53**, 545 (1973).

[31] A. Afanasev, I. Akushevich, and N.P. Merenkov, e-Print: hep-ph/0208260.

[32] T. Powell, *et al.* Phys. Rev. Lett. **24**, 753 (1970).

[33] X. Jiang *et al.*, Measurement of Target Single Spin Asymmetry in Elastic $ep^{\uparrow}$ scattering, proposal to PAC-25.

[34] S.P. Wells, *et al.*, Phys. Rev. C. **63**, 064001 (2001).

[35] M.J. Alguard *et al*, Phys. Rev. Lett. **37**, 1258 (1976).

[36] B.M. Preedom and R. Tegen, Phys. Rev. C **36**, 2466 (1987).

[37] Uncertainties on the beam-line instrumentation, if not explicitly specified, are values that were routinely achieved in Hall C.

[38] D. Day, JLab E93-026, The Charge Form Factor of the Neutron.

[39] O. Rondon-Aramayo, JLab E01-006, Precision Measurement of the Nucleon Spin Structure Functions in the Region of the Nucleon Resonances.

[40] M. Steinacher, I. Sick, Nucl. Inst. Meth. A **455**, 759 (2000).

[41] O.A. Rondon, Z.-E. Meziani, S. Choi and G. Warren, O.A. Rondon, JLab E01-109, Spin Asymmetries on the Nucleon Experiment (SANE)

[42] A. Dzierba and J. Napolitano, JLab E94-016, A Measurement of Rare Radiative Decays of the ϕ Meson.

[43] R. Crittendon *et al.*, Nucl. Instrum. Method A **387**, 377 (1997).

[44] E. Frlez, D. Pocanic, *et al.*, RadPhi Calorimeter Gain Monitoring System, http://www.jlab.org/ choi/Sane/Frlez.pdf

[45] G. Cates, K. McCormick, B. Reitz, B. Wojtsekhowski, JLab E02-013, Measurement of the Neutron Electric Form Factor G_E^n at High Q^2.

[46] K. McCormick's talk, G_E^n Collaboration Meeting Minutes, May 29, 2003. http://hallaweb.jlab.org/experiment/E02-013/collabmeetings/may2003/detrate.ps.gz

[47] G. Warren, O. Rondon, F. Wesselmann and M. Zeier, *Uncertainties in the Beam Charge Asymmetry for Gen01*, report to the E93-026 collaboration, (Sept.20, 2002).

[48] K. Sugimoto, Phys. Rev. **182**, 1051 (1969).

[49] O.A. Rondon, Phys. Rev. C **60**, 035201 (1999).

[50] J.W. Lightbody, Jr., J.S. O'Connell, Computers in Physics, May/June (1988);

[51] P. Bosted, Phys. Rev. C **51**, 409 (1995).

[52] T.W. Donnelly and A.S. Raskin, Annals of Phys., **169**, 247 (1986).

[53] Report of the Jan 12-16, 2004 Meeting of the Jefferson Lab Program Advisory Committee PAC 25.